DOI: 10.1002/ejoc.200800301

4′-Hydrazone Derivatives of 2,2′:6′,2"-Terpyridine: Protonation and Substituent Effects

Jonathon E. Beves,[a] Edwin C. Constable,*[a] Catherine E. Housecroft,*[a] Markus Neuburger,[a] Silvia Schaffner,[a] and Jennifer A. Zampese[a]

Keywords: Hydrazone / Protonation / Rotamers / 2,2′:6′,2"-Terpyridine

Four 4′-hydrazone derivatives of 2,2′:6′,2"-terpyridine which vary in their *N*- and *C*-substitution in the R′NN=CRPh unit have been prepared and structurally characterized. Protonation studies and solution behaviour of these compounds are described, as well as representative crystal structures of mono- and diprotonated derivatives. In the solid-state structures of each neutral compound, the tpy domain adopts the anticipated *trans*,*trans*-conformation, and intramolecular steric factors compete with π-stacking effects to control the amount to which the *C*-phenyl substituent twists out of the plane of the tpy unit. When R′ = H, the imine NH group engages in hydrogen bonding interactions in the solid state, except where R = Ph. In solution, variable temperature ^{1}H NMR spectroscopy shows that on going from R = Me to Ph (with R′ = H), the barrier to rotation about the C_{py}–N_{imine} bond increases; with R = R′ = H, the hydrogen bonding capabilities of the solvent to the imine NH influence this dynamic process. In the *N*-methyl derivative (R = H and R′ = Me), rotation about the C_{py}–N_{imine} bond is facile at room temperature. Protonation of the derivative with R = R′ = H results in an increase in the activation barrier to rotation, consistent with a greater π-contribution to the C_{py}–N_{imine} bond.

Introduction

The chemistry of hydrazones and their metal complexes has long been an area of active interest, because of their properties appropriate for their applications in, for example, sensors, non-linear optical and polymeric materials[1–6] and their biological applications.[7–10] Within supramolecular chemistry, Lehn has incorporated hydrazone units into pyrimidine- and pyridine-containing molecular strands that undergo programmed self-organization into metal-free helical architectures[11–13] and metal-containing helical wires[14,15] or grid-like arrays.[16–22] Among the latter are $[Co_4L_4]^{8+}$ complexes [L = 4,6-bis(benzylidenehydrazino)-2-phenylpyrimidine or 2-phenylpyrimidine-4,6-dicarbaldehyde bis(phenylhydrazone)] in which the eight hydrazone NH protons can be sequentially and reversibly removed in pH-dependent steps resulting in significant changes in the absorption spectra of the complexes.[18]

We have recently reported a series of $[FeL_2]^{2+}$ and $[RuL_2]^{2+}$ complexes in which L is 4′-(2-pyridyl)-, 4′-(3-pyridyl)- or 4′-(4-pyridyl)-2,2′:6′,2"-terpyridine, and have described the effects of mono- and bis-*N*-methylation on the absorption spectra and electrochemical properties of these complexes.[23] As an extension of this work, we have investigated the 4′-(3,5-dimethylpyrazol-1-yl)-2,2′:6′,2′′-terpyridine ligand and its complex formation,[24] and in the first of a series of papers, we now report the formation of four 4′-hydrazone derivatives of 2,2′:6′,2′′-terpyridine (compounds **1**–**4**, Scheme 1) and describe structural aspects and solution behaviour of these compounds and their conjugate acids. In future papers, we will turn our attention to the coordination behaviour of these and related ligands. However, it is initially important for us to understand how the free ligands behave in solution.

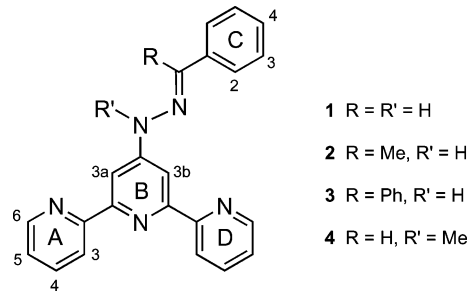

Scheme 1. Structures of ligands **1**–**4** and labelling used for the NMR spectroscopic assignments. Rings A and D, and protons H^{B3a} and H^{B3b} are only distinguished on the NMR timescale at low temperature (see text). For compound **3**, the second phenyl substituent is ring E.

[a] Department of Chemistry, University of Basel,
Spitalstrasse 51, 4056 Basel, Switzerland
Fax: +41-61-267-1018
E-mail: catherine.housecroft@unibas.ch
Supporting information for this article is available on the WWW under http://www.eurjoc.org or from the author.

Results and Discussion

Syntheses and Structural Studies

The synthetic route to hydrazones **1**–**4** (Scheme 1) was by the well established acid-catalysed condensation of a hydrazine (4′-hydrazino-2,2′:6′,2′′-terpyridine or 4′-(1-methylhydrazino)-2,2′:6′,2′′-terpyridine[25–27]) and an aldehyde or ketone (benzaldehyde for **1** and **4**, acetophenone for **2**, and benzophenone for **3**). The reaction of 4′-hydrazino-2,2′:6′,2′′-terpyridine and benzaldehyde in methanol in the presence of a few drops of concentrated H_2SO_4 resulted in the formation of a bright yellow solid, elemental analysis of which was consistent with the methyl sulfate salt of $[H_2\mathbf{1}]^{2+}$ (Scheme 2). This observation is reminiscent of the formation of methyl sulfate and ethyl sulfate salts of diprotonated 4′-(3,5-dimethylpyrazol-1-yl)-2,2′:6′,2′′-terpyridine when 4′-hydrazino-2,2′:6′,2′′-terpyridine reacts with pentane-2,4-dione in MeOH or EtOH in the presence of concentrated H_2SO_4.[24] The electrospray mass spectrum of $[H_2\mathbf{1}][MeOSO_3]_2$ was unhelpful in confirming the protonation state of **1**, showing evidence only for the $[H\mathbf{1}]^+$ ion (*m*/*z* 352). The room temperature ^1H NMR spectrum in [D$_6$]DMSO showed the presence of methyl protons at δ 3.38 and 3.15 ppm. The latter was assigned to MeOH[28] and the former to the $[MeOSO_3]^-$ ion. The combined relative integrals for the methyl proton signals with respect to signals for the tpy protons were consistent with the formulation $[H_2\mathbf{1}][MeOSO_3]_2$. In the ^{13}C NMR spectrum ([D$_6$]DMSO), signals at δ 48.6 and 53.0 ppm were assigned to MeOH[28] and $[MeOSO_3]^-$, respectively. We attribute the presence of the MeOH (always present to some extent in [D$_6$]DMSO solutions of the sample) to hydrolysis of $[MeOSO_3]^-$ by residual water in the solvent.[24,29] When the reaction of 4′-hydrazino-2,2′:6′,2′′-terpyridine and benzaldehyde was carried out in methanol in the presence of a few drops of concentrated HNO_3 or HCl, a bright yellow solid was isolated in each case. [D$_6$]DMSO solutions of these products exhibited the same ^1H NMR spectroscopic signatures for the tpy unit as in $[H_2\mathbf{1}][MeOSO_3]_2$, suggesting the formation of $[H_2\mathbf{1}][NO_3]_2$ and $[H_2\mathbf{1}]Cl_2$. In each salt, the signal for protons H^{A3} and H^{B3} are either very broad or are not observed at 295 K. We return to a more detailed discussion of the NMR spectra later.

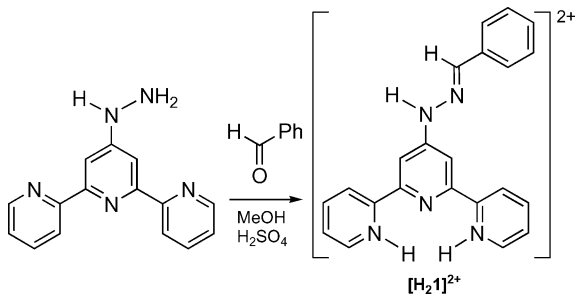

Scheme 2. Formation of $[H_2\mathbf{1}]^{2+}$ as the methyl sulfate salt.

The salts $[H_2\mathbf{2}][MeOSO_3]_2$, $[H_2\mathbf{3}][MeOSO_3]_2$ and $[H_2\mathbf{4}][MeOSO_3]_2$ (all bright yellow solids) were made in an analogous manner to $[H_2\mathbf{1}][MeOSO_3]_2$. Although the electrospray mass spectrum of these salts provided evidence only for $[H\mathbf{2}]^+$ (*m*/*z* 366), $[H\mathbf{3}]^+$ (*m*/*z* 428) and $[H\mathbf{4}]^+$ (*m*/*z* 366), respectively, the NMR spectroscopic data were consistent with the formation of $[H_2\mathbf{2}][MeOSO_3]_2$, $[H_2\mathbf{3}][MeOSO_3]_2$ and $[H_2\mathbf{4}][MeOSO_3]_2$. However, as with $[H_2\mathbf{1}][MeOSO_3]_2$, hydrolysis of the anion by water in the [D$_6$]DMSO solvent led to the presence of MeOH in addition to $[MeOSO_3]^-$.

Treatment of each of aqueous solutions of $[H_2\mathbf{1}][MeOSO_3]_2$, $[H_2\mathbf{2}][MeOSO_3]_2$, $[H_2\mathbf{3}][MeOSO_3]_2$ and $[H_2\mathbf{4}][MeOSO_3]_2$ with excess $NaBF_4$ led to the formation of pale yellow $[H\mathbf{1}][BF_4]$, $[H\mathbf{2}][BF_4]$, $[H\mathbf{3}][BF_4]$ and $[H\mathbf{4}][BF_4]$, respectively. Changes in the NMR spectroscopic data were consistent with the conversion of each diprotonated to monoprotonated tpy species. For example, a comparison of the ^{13}C NMR spectra (in [D$_6$]DMSO) revealed that signals for carbons C^{A4} and C^{A5} shifted to lower frequency upon reaction of $[H_2\mathbf{1}][MeOSO_3]_2$ with $[BF_4]^-$; $\Delta\delta$ = 0.6 and 0.3 ppm for C^{A4} and C^{A5}, respectively where $\Delta\delta = \delta([MeOSO_3]^-$ salt – $[BF_4]^-$ salt). Similarly, although the signal for C^{A3} is broad, a change in chemical shift to lower frequency is observed. The addition of NH_4PF_6 to an aqueous solution of $[H_2\mathbf{1}][MeOSO_3]_2$ yielded, after purification, a pale yellow solid product, analytical data for which were consistent with $[H\mathbf{1}][PF_6]$. The aromatic region of the ^{13}C NMR spectrum of a [D$_6$]DMSO solution of the hexafluorophosphate salt was essentially identical to that of the tetrafluoroborate salt. Detailed discussion of the ^1H NMR spectra is given later.

The reactions of $[H_2\mathbf{1}][MeOSO_3]_2$, $[H_2\mathbf{2}][MeOSO_3]_2$, $[H_2\mathbf{3}][MeOSO_3]_2$ and $[H_2\mathbf{4}][MeOSO_3]_2$ with K_2CO_3 allowed the neutral compounds **1**, **2**, **3** and **4** to be isolated. All compounds have been fully characterized by electrospray mass spectrometry, elemental analysis, ^1H and ^{13}C NMR spectroscopy and single-crystal X-ray crystallography. In the ^1H NMR spectra, the loss of the resonance for the methyl sulfate anion was consistent with the formation of each neutral product. Colourless plates of **1** were grown by slow evaporation of a $CHCl_3$ solution of the compound. Figure 1 shows the molecular structure of **1**, with the tpy unit in the anticipated *trans*,*trans*-conformation with typical bond lengths and angles. The aromatic rings are significantly twisted with respect to one another [angles between the least-squares planes of rings containing N1 and N2, N2 and N3, and N2 and C17: 10.64(7), 20.87(7) and 24.26(8)°]. The substituents around the C=N bond adopt an (*E*)-configuration. In crystalline **1**, pyridine nitrogen atom N3 acts as a hydrogen-bond acceptor and pairs of molecules of **1** associate as shown in Figure 2 (a). The evolution of the two symmetry related N4–H1···N3^i interactions leads to the formation of weaker $CH_{imine}\cdots N_{pyridine}$ interactions as well as a repulsive H91···H91^i contact (2.38 Å). The V-shaped dimeric motifs assemble as shown in Figure 2 (b), forming interlocking zigzig chains which run parallel to the crystallographic *c*-axis.

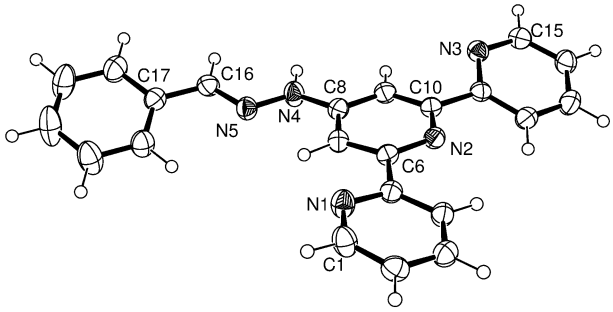

Figure 1. The molecular structure of **1** with thermal ellipsoids plotted at the 50% probability level. Selected bond lengths and angles: N4–C8 1.379(2), N4–N5 1.371(2), N5–C16 1.282(2), C16–C17 1.457(2) Å, N5–N4–C8 119.4(1), N4–N5–C16 116.6(1), N5–C16–C17 121.2(2)°.

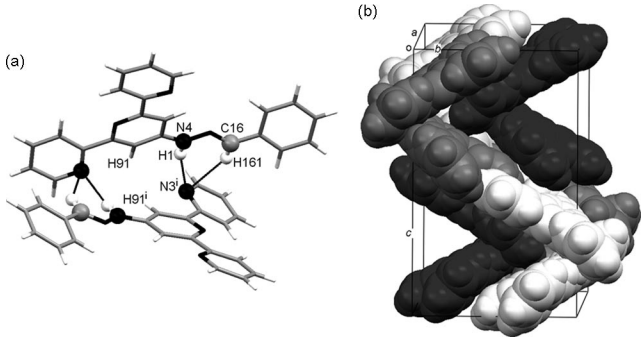

Figure 2. (a) Hydrogen bond association between pairs of molecules of **1** in the solid state. Parameters: N4H1···N3^{i} 2.19 Å, N4···N3^{i} 3.091(2), N4–H1···N3^{i} 156°. C16H161···N3 2.62 Å, C16···N3 3.482(2) Å, C16–H161···N3 144°. Symmetry code i = 2 – *x*, *y*, 1/2 – *z*. (b) Assembly of hydrogen-bonded dimers of **1** in the solid state.

X-ray-quality colourless plates of **2** (Figure 3) were grown by slow evaporation of a CH_2Cl_2 solution of the compound. Bond lengths and angles are unexceptional, the tpy unit has the usual *trans*,*trans*-conformation, and the hydrazone adopts an (*E*)-configuration. The angles between the least-squares planes of the rings containing N1 and N2, N2 and N3, and N2 and C17 are 6.06(7), 6.44(7) and 67.5(8)°, and therefore a molecule of **2** is much closer to being planar than is **1**. This is, presumably, a consequence of the packing which is dominated by π-stacking (Figure 4). Pairs of molecules stack in slightly offset columns with a distance of 3.20 Å between the least-squares planes of the molecules. The columns interlock as shown in Figure 4. The packing efficiency of the crystalline lattice is 70.5%,[30] and the stabilizing energy gained from the extensive π-stacking must compensate for the repulsive energy of the close $C_{tpy}H\cdots CH_3$ contacts within each pair of molecules (H91···H173^{i} = 2.37 Å, symmetry code i = 1 – *x*, 2 – *y*, 1 – *z*). The mode by which efficient packing is achieved by **2** contrasts with that in **1** (packing efficiency of 69.9%[30]) in which $NH_{imine}\cdots N_{pyridine}$ and $CH_{imine}\cdots N_{pyridine}$ interactions are important (Figure 2). In **2**, the steric requirements of the methyl substituents presumably prevent the evolution of efficient $NH_{imine}\cdots N_{pyridine}$ interactions, with the result that hydrogen bonding interactions are less favourable than in **1**.

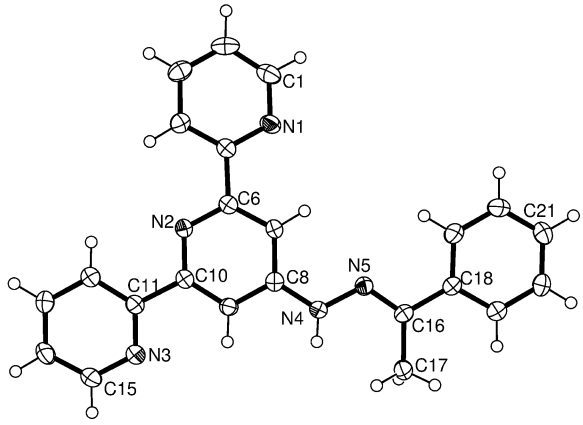

Figure 3. The molecular structure of **2** with thermal ellipsoids plotted at the 50% probability level. Selected bond lengths and angles: N4–C8 1.378(2), N4–N5 1.364(2), N5–C16 1.293(2), C16–C17 1.502(2), C16–C18 1.483(2) Å, N5–N4–C8 120.2(1), N4–N5–C16 118.2(1), N5–C16–C17 124.3(1), N5–C16–C18 115.9(1)°.

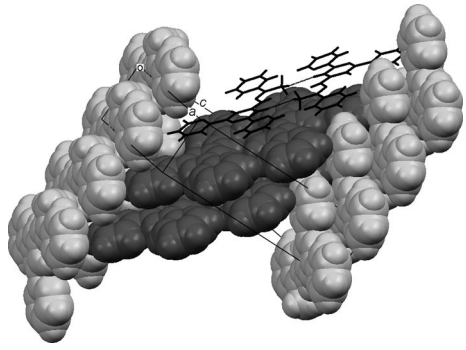

Figure 4. Packing diagram for **2** showing interlocking π-stacked pairs of molecules. One pair is shown in stick representation, and illustrates the close $C_{tpy}H\cdots CH_3$ contacts.

Crystals of **3**.CH_2Cl_2 suitable for X-ray diffraction were grown by by slow evaporation of a CH_2Cl_2 solution of the compound. Figure 5 illustrates that the tpy domain is close to being planar [angles between the least-squares planes of rings containing N1 and N2, and N2 and N3: 2.51(8) and 6.74(8) Å] and adopts the expected *trans*,*trans*-conformation. The phenyl substituents are twisted away from the plane of the hydrazone unit [angles between the least-squares planes of rings containing N2 and C17, and N2 and C23: 19.15(8) and 75.01(8)°], thus minimizing steric interactions. It is worth noting that the imine hydrogen atom H4 is in close contact with the *ipso*-carbon atom C23 (H4···C23 2.42 Å) and the adjacent C28 (H4···C28 2.67 Å), a situation discussed previously by Drew et al.[31] The molecules pack so that pairs of tpy units are π-stacked, with the planes of pyridine rings containing N2 and N3 being 3.58 Å apart. The solvent CH_2Cl_2 molcules reside in cavities, hy-

drogen bonded to pyridine N atoms [C29H292···N3 2.45 Å, C29···N3 3.273(3) Å, C29–H292···N3 143°. C29H291···N2^{i} 2.55 Å, C29···N2^{i} 3.417(3) Å, C29–H292···N2^{i} 153°; symmetry code i = 1 – *x*,1 – *y*, 1 – *z*] and with additional weak contacts to phenyl rings (Cl1···H21^{ii} 2.94 Å, symmetry code ii = –1 + *x*, –1 + *y*, *z*; Cl1···centroid ring containing C23 3.79 Å). Presumably, the proximity of a phenyl substituent to the imine NH group prevents the latter engaging in hydrogen bonded interactions. The closest approach of one CH_2Cl_2 chlorine atom is 3.26 Å (N4H4···Cl1).

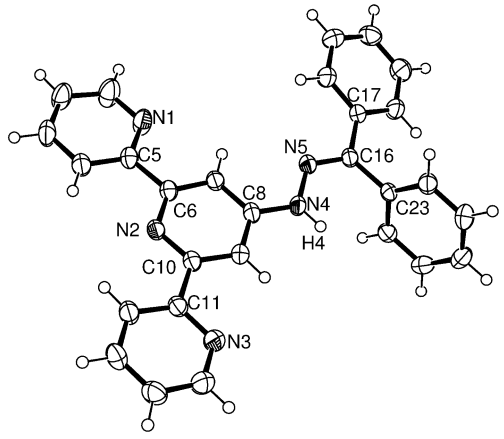

Figure 5. The molecular structure of **3** in **3**.CH_2Cl_2 with thermal ellipsoids plotted at the 50% probability level. Selected bond lengths and angles: N4–C8 1.378(2), N4–N5 1.361(2), N5–C16 1.288(2), C16–C17 1.479(2), C16–C23 1.495(2) Å; N5–N4–C8 118.5(1), N4–N5–C16 118.6(1), N5–C16–C17 116.2(1), N5–C16–C23 123.9(1)°.

In each of compounds **1** to **3**, the hydrazone unit contains an NH unit which has the potential to engage in hydrogen bonded interactions, although in **3** this appears to be unfavourable on steric grounds (see above). The deviation of the HNN=C framework from the plane of the central pyridine ring of the tpy domain in each compound is small. Each compound exhibits the same C_{py}–N_{imine} bond length (see Figure captions) and this is shorter than the sum of the covalent radii (1.52 Å) indicating that the bond contains some π-character.

X-ray-quality crystals of **4** were grown by by slow evaporation of a CH_2Cl_2/EtOH solution of the compound, allowing us to investigate the structural consequences of introducing an *N*-methyl substituent. The structure of **4** is shown in Figure 6; bond parameters are as expected and the substituents about the C=N bond adopt an (*E*)-configuration. The tpy domain has the anticipated *trans*,*trans*-conformation, and deviates slightly from planarity [angles between the least-squares planes containing N1 and N2, and N2 and N3: 9.45(9) and 9.00(9)°, respectively]. The phenyl substituent is twisted out of the plane of the central pyridine ring by 20.42(9)°. The deviation of the N5N4C16 unit from the least-squares plane of the ring containing N2 is only 11.4(2)°, compared to a corresponding angle of 7.4(2)° for compound **1**. This results in repulsive H_{Me}···H_{py} contacts, but this is presumably offset by retention of some π-character in the C8–N4 bond [1.389(2) Å compared to 1.378(2) or 1.379(2) Å in **1**–**3**]. Other simple *N*-methyl hydrazones also show this preference.[32–35] Pairs of molecules (related by a crystallographic inversion centre) assemble so that the pyridine rings containing N2 are π-stacked (distance between planes of rings: 3.36 Å). Atom N2 makes a weak contact to a phenyl CH group in an adjacent pair of molecules (N2···H231^{i}C23^{i} 2.70 Å, symmetry code i = $^{1}/_{2}$ + *x*, $^{3}/_{2}$ –*y*, $^{1}/_{2}$ + *z*).

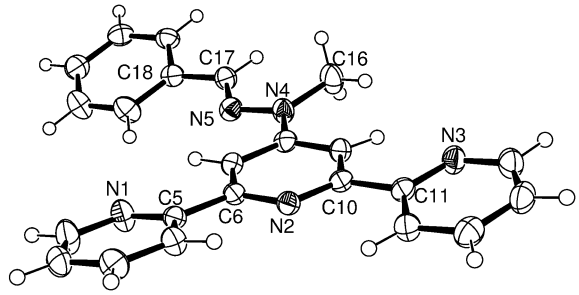

Figure 6. The molecular structure of **4** with thermal ellipsoids plotted at the 50% probability level. Selected bond lengths and angles: N4–C8 1.389(2), N4–N5 1.363(2), N5–C17 1.284(2), N4–C16 1.450(2), C17–C18 1.466(3) Å; N5–N4–C8 115.8(1), N4–N5–C17 119.1(2), N5–C17–C18 120.2(2)°.

The mono- and diprotonated states of the 4′-hydrazone derivatives of 2,2′:6′,2′′-terpyridine were confirmed by representative structural studies. X-ray-quality crystals of [H_2**1**]Cl_2·DMSO were grown from a DMSO solution of the compound. Figure 7 shows the $[H_2\mathbf{1}]^{2+}$ cation, hydrogen bonded to the two chloride ions in the asymmetric unit. The tpy domain adopts a *cis*,*cis*-configuration. In an $[H_2tpy]^{2+}$ ion, it is usual for the two outer pyridine rings to carry one proton each and for the latter to be involved in hydrogen-bonded interactions with the central pyridine *N*-atom as well as with an acceptor atom.[36–42] As Figure 7 illustrates, the $[H_2\mathbf{1}]^{2+}$ ion in [H_2**1**]Cl_2·DMSO falls into this structural pattern, with one chloride ion acting as a hydrogen-bond acceptor with respect to the $[H_2\mathbf{1}]^{2+}$ ion. The imine NH also acts as a hydrogen-bond donor, interacting with the second chloride ion (see Figure caption). The hydrogen-bonded motif locks the tpy unit into a near planar conformation [angles between the least-squares planes of the rings containing N1 and N2, and N2 and N3 are 9.90(7) and 7.72(7)°, respectively]. The phenyl substituent also lies close to this plane [angle between the least-squares planes of rings containing N1 and C17: 8.95(8)°]. The latter is a consequence of the molecular packing; $[H_2\mathbf{1}]^{2+}$ cations assemble into π-stacked columns with alternating distances of 3.19 and 3.49 Å between the least-squares planes drawn through adjacent cations. The packing is completed by extensive hydrogen bonding interactions involving the chloride ions and DMSO solvent molecules.

Yellow plates of [H_2**2**][NO_3][$MeOSO_3$]·H_2O were grown by adding a drop of dilute aqueous HNO_3 to an aqueous solution of [H_2**2**][$MeOSO_3$]$_2$ and allowing the solvent to evaporate slowly. A single-crystal X-ray diffraction study

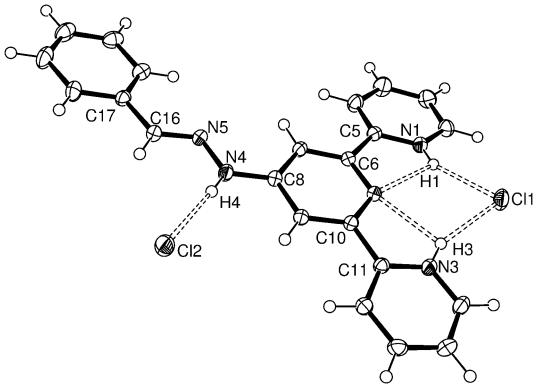

Figure 7. The molecular structure of $[H_2\mathbf{1}]Cl_2$ in the asymmetric unit of $[H_2\mathbf{1}]Cl_2$·DMSO with thermal ellipsoids plotted at the 50% probability level. Selected bond lengths and angles: N4–C8 1.362(2), N4–N5 1.367(2), N5–C16 1.290(2), C16–C17 1.465(2) Å; N5–N4–C8 119.7(1), N4–N5–C16 115.0(1)°. Hydrogen bond parameters: N1H1···Cl1 2.26 Å, N1···Cl1 3.018(1) Å, N1–H1···Cl1 151°; N3H3···Cl1 2.25 Å, N3···Cl1 3.049(1) Å, N3–H3···Cl1 154°; N1H1···N2 2.26 Å, N1···N 2.619(2) Å, N1–H1···N2 106°; N3H3···N2 2.30 Å, N3···N2 2.638(2) Å, N3–H3···N2 104°; N4H4···Cl2 2.29 Å, N3···N2 3.158(2), N3–H3···N2 173°.

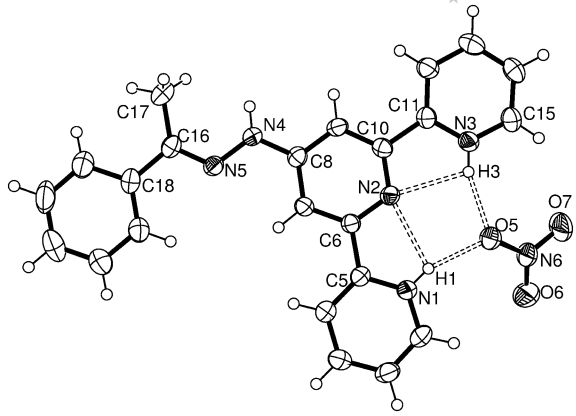

Figure 8. The molecular structure of the $[H_2\mathbf{2}]^{2+}$–$[NO_3]^-$ hydrogen-bonded ion pair in $[H_2\mathbf{2}][NO_3][MeOSO_3]\cdot H_2O$; thermal ellipsoids are plotted at the 50% probability level. Selected bond lengths and angles: C8–N4 1.377(4), N4–N5 1.363(3), C16–N5 1.299(4), C16–C17 1.494(4), C16–C18 1.492(4) Å, C8–N4–N5 118.9(2), N4–N5–C16 118.6(2), C18–C16–N5 115.2(3), C17–C16–N5 123.9(3), C17–C16–C18 120.9(3)°. See text for the hydrogen bond parameters.

confirmed that **2** is diprotonated (Figure 8). The three pyridine rings adopt a *cis,cis*-configuration, with the nitrate ion acting as a hydrogen-bond acceptor [N1H1···O5 1.92 Å, N1···O5 2.722(3) Å, N1–H1···O5 161°; N3H3···O5 1.95 Å, N3···O5 2.762(3) Å, N3–H3···O5 161°]. As in $[H_2\mathbf{1}]^{2+}$, this hydrogen bonding compels the tpy unit in $[H_2\mathbf{2}]^{2+}$ to be planar [angles between the least-squares planes of the rings containing N1 and N2, and N2 and N3: 2.7(1) and 4.6(1)°, respectively]. The diprotonated state of the tpy derivative is further stabilized by hydrogen-bonded interactions to N2 [N3H3···N2 2.29 Å, N3···N2 2.660(3) Å, N3–H3···N2 107°; N1H1···N2 2.29 Å, N1···N2 2.670(3) Å, N1–H1···N2 107°]. The imine NH group is hydrogen-bonded to atom O4 of the $[MeOSO_3]^-$ anion [N4H4···O2 2.04 Å, N4···O2 2.859(4) Å, N4–H4···O2 161°]. The hydrogen-bonded interactions are further extended to the solvate water molecule and then, via a crystallographic inversion centre, to a repeat unit (Figure 9). The phenyl ring is essentially coplanar with the tpy unit [angle between the least-squares planes of the C_6 ring and ring containing N2: 6.2(2)°]. The $[H_2\mathbf{2}]^{2+}$ cations are stacked in the crystal lattice to generate a herringbone architecture (Figure S1) consisting of alternating layers with separations (calculated for least square planes through each molecule) of 3.22 and 3.48 Å. The shorter of these separations arises from π-stacking between pyridine rings containing atoms N2 and N3, whereas C_{methyl}···$py_{centroid}$ interactions (C17···centroid of ring containing N1: 3.55 Å) give rise to the larger layer spacing.

Attempts to grow crystals of yellow $[H_2\mathbf{3}][MeOSO_3]_2$ by slow evaporation of an aqueous solution of the salt instead gave rise to X-ray-quality colourless plates of $[H\mathbf{3}][MeOSO_3]$. The structure of the $[H\mathbf{3}]^+$ cation is shown in Figure 10. The tpy domain is close to being planar [angles between the least-squares planes of rings containing atoms N1 and N2, and N2 and N3: 2.8(1) and 11.42(9)°,

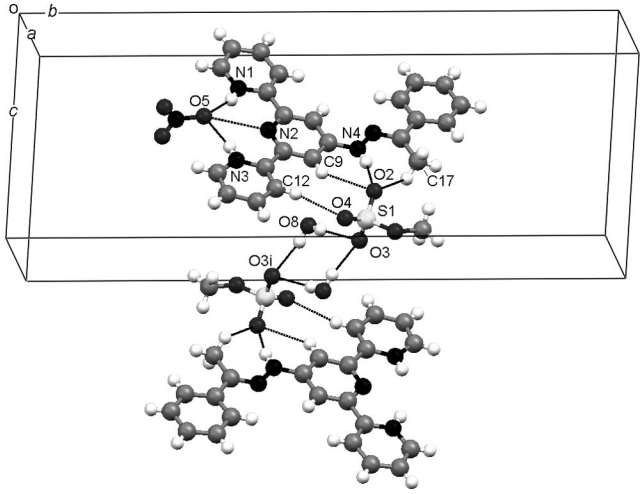

Figure 9. Part of the hydrogen-bonded network in $[H_2\mathbf{2}][NO_3]$-$[MeOSO_3]\cdot H_2O$; symmetry code i = 1 – *x*, 1 – *y*, 2 – *z*. N and O atoms are shown in black. Parameters for hydrogen bonded interactions is given in Table S1 (see Supporting Information).

respectively]. It adopts a *cis,cis*-conformation, with both of atoms N1 and N3 participating in hydrogen-bonded interactions with the N2H2 unit [see discussion of $(H\mathbf{1})^+$ and $(H\mathbf{2})^+$]. The deviations of atoms N4, N5 and C16 from the least-squares plane of the central pyridine ring are 0.08, 0.11 and 0.41 Å, respectively. Neither phenyl substituent is coplanar with the central pyridine ring [angles between the least-squares planes of the rings containing C17 and N2, and C23 and N2: 23.6(1) and 64.2(1)°, respectively]. In the crystal lattice, cations are arranged in head-to-tail pairs with π-stacking of the central rings of the tpy units (distance between rings containing atoms N2: 3.40 Å). This results in unfavourable H11···H251[a] contacts (2.2 Å, symmetry code *a* = –*x*, 1 – *y*, 1 – *z*). The cation pairs assemble into columns, with adjacent pairs being slightly offset from one another. Anions and cations are associated through hy-

drogen bonding, with the imine NH acting as the hydrogen-bond donor [N4H4···O3 1.89 Å, N4···O3 2.789(2) Å, N4–H4···O3 151°].

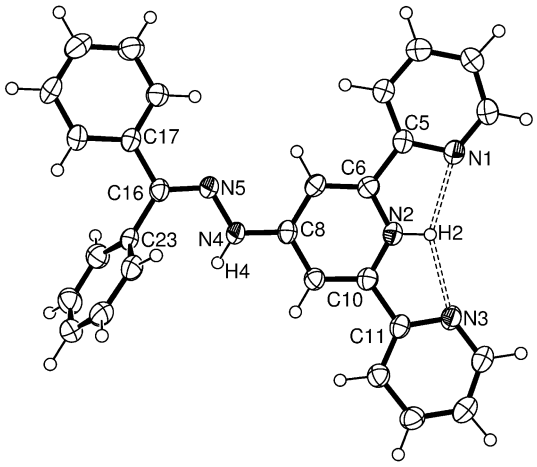

Figure 10. The molecular structure of the [H**3**]$^+$ cation in [H**3**][$MeOSO_3$]; thermal ellipsoids are plotted at the 50% probability level. Selected bond lengths and angles: N4–N5 1.376(2), N4–C8 1.348(2), N5–C16 1.292(2), N2–H2 0.98, N1···H2 2.20, N3···H2 2.25, N1···N2 2.630(2), N2···N3 2.650(2) Å; N5–N4–C8 118.8(2), N4–N5–C16 117.1(2)°.

The change in protonation state that accompanies dissolution of [H_2**1**][$MeOSO_3$]$_2$ or [H_2**2**][$MeOSO_3$]$_2$ in hot MeOH followed by anion exchange, was confirmed by single crystal structure determinations of [H**2**][BF_4] [colourless plates grown by slow evaporation of an aqueous acetone (1:5) solution of the salt] and of [H**1**][PF_6]·H_2O [colourless plates obtained by slow evaporation of a MeCN/H_2O (5:1) solution of the compound]. Figure 11 and Figure 12 show the molecular structures of the [H**2**]$^+$ and [H**1**]$^+$ ions present in [H**2**][BF_4] and [H**1**][PF_6]·H_2O, respectively. In both salts and in [H**3**][$MeOSO_3$], the tpy unit adopts a *cis*,*cis*-conformation. This is in contrast to the *cis*,*trans*-conformation observed in [Htpy][CF_3SO_3][43] and [Htpy][ReO_4].[44] In these salts, a [CF_3SO_3]$^-$ or [ReO_4]$^-$ anion resides close to the site of protonation in the cation and participates in a hydrogen-bonded interaction which is in addition to the N–H···N interaction responsible for the *cis*-arrangement of two of the pyridine rings. A pertinent difference between [Htpy]$^+$ and the family of monoprotonated tpy ligands in this study is the presence of the hydrazone NH group which may also become involved in hydrogen bonding. In [H**3**][$MeOSO_3$], the hydrazone NH group in the [H**3**]$^+$ cation is hydrogen bonded to the methyl sulfate anion [N4–H4 0.98, N4H4···O3 1.89, N4···O3 2.789(2), N4–H4···O3 151°]. Similarly, in [H**2**][BF_4], the hydrazone NH group participates in hydrogen bonding to the [BF_4]$^-$ counterion (see later). In [H**1**][PF_6]·H_2O, the hydrazone NH is hydrogen bonded to the solvate water molecule [N4H2···O1 1.93 Å, N4···O1 2.806(5) Å, N4–H2···O1 178°], and the latter forms weak hydrogen bonds to the [PF_6]$^-$ anion. We propose that the [H**1**]$^+$, [H**2**]$^+$ and [H**3**]$^+$ cations adopt *cis*,*cis*-conformations in order that both of the outer pyridine *N*-atoms may be involved in stabilizing hydrogen-bonded interactions with the NH unit, while the counterions or solvate are preferentially involved in hydrogen bonding with the hydrazone NH. The two outer pyridine rings in each of the [H**2**]$^+$ and [H**1**]$^+$ cations are twisted out of the plane of the central ring with angles between the least-squares planes of the rings containing N1 and N2, and N2 and N3 of 10.8(1) and 6.5(1)° in [H**2**][BF_4], and 7.2(2) and 16.3(2)° in [H**1**][PF_6]·H_2O. The phenyl ring in [H**2**][BF_4] is not coplanar with the central pyridine ring [angle between the least-squares planes: 18.4(9)°]. This results in a reduction in the conjugation along the C8N4N5C16C18 chain, which manifests itself in a longer C_{phenyl}–$C_{azomethine}$ bond [1.483(3) Å] compared to that in [H**1**][PF_6]·H_2O [1.457(6) Å] in which the phenyl and central pyridine rings are coplanar [angle between least-squares planes: 0.7(2)°]. The difference between the molecular structures of the cations appears to be associated with the crystal packing. In [H**1**][PF_6]·H_2O, cations are stacked with alternating separations of 3.29 and 3.32 Å. This pattern arises from the interactions of each phenyl ring with an imino nitrogen atom (N5) on one side and a π-stacked pyridine ring (containing N2) on the other. The overall packing can be described in terms of stacks of cations, between which run columns of water molecules and [PF_6]$^-$ anions (Figure S2, Supporting Information). In contrast, the packing motif in [H**2**][BF_4] consists of pairs of [H**2**]$^+$ cations related by a C_2 axis (Figure S3). There is π-stacking between pairs of pyridine rings containing N3 (distance between planes: 3.35 Å) and N2 (distance between planes: 3.31 Å). The cavity formed by the hydrazone NH and methyl group accommodates a [BF_4]$^-$ ion with associated hydrogen-bonded interactions [N4···F2^i 2.798(4) Å, N4–H4···F2^i 148°; C4···F1 3.337(3) Å, C4–H41···F1^i 172°; C7···F1^i 3.359(3) Å, C7–H71···F1^i 171°; C17···F2^i

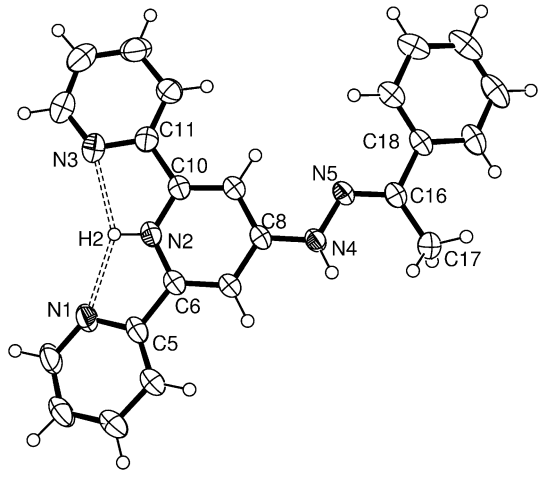

Figure 11. The molecular structure of the [H**2**]$^+$ cation in [H**2**][BF_4] with thermal ellipsoids plotted at the 50% probability level. Selected bond lengths and angles: N4–C8 1.355(2), N4–N5 1.372(2), N5–C16 1.289(2), C16–C17 1.500(3), C16–C18 1.483(3), N2–H2 0.92, N1···H2 2.18, N3···H2 2.23, N1···N2 2.615(3), N2···N3 2.616(3) Å, N5–N4–C8 117.3(2), N4–N5–C16 118.8(2), N5–C16–C17 124.9(2), N5–C16–C18 114.2(2), C17–C16–C18 120.9(2)°.

3.427(4) Å, C17–H173···F2^{i} 163°; symmetry code i = x, 1 – y, $^{1}/_{2}$ + z]. The packing is then further extended through aromatic CH···F interactions and stacking of dimeric motifs.

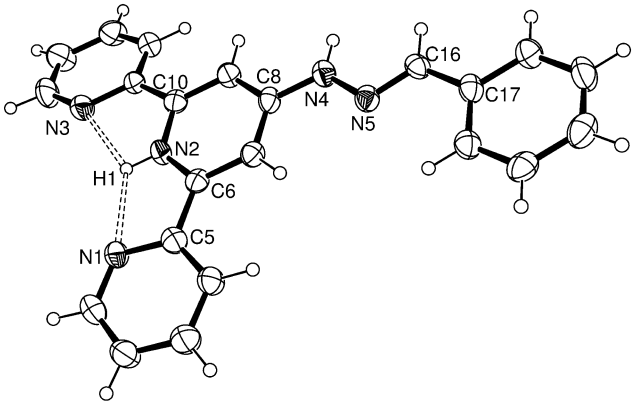

Figure 12. The molecular structure of the [H**1**]$^{+}$ cation in [H**1**][PF_6]·H_2O with thermal ellipsoids plotted at the 40% probability level. Selected bond lengths and angles: C8–N4 1.346(5), N4–N5 1.377(5), C16–N5 1.284(5), C16–C17 1.457(6), N2–H1 0.89, N1···H1 2.24, N3···H1 2.25, N1···N2 2.636(5), N2···N3 2.653(5) Å, C8–N4–N5 119.8(3), N4–N5–C16 115.5(3), C17–C16–N5 121.2(4)°.

Solution Behaviour

In solution, each of compounds **1** to **4** exists as a single isomer, shown by NOESY experiments to be the (*E*)-isomer as observed in the solid state. This is the expected isomer for aryl hydrazones.[45] The ^{1}H NMR spectra of compounds **1** to **4** and of their protonated analogs are instructive in terms of the following two fluxional processes: (i) rotation about the C_{py}–N_{imine} bond, and (ii) rotation about the C_{py}–C_{py} bonds. We first consider the ^{1}H NMR spectra of the neutral compounds, shown in Figure 13. In [D_6]DMSO, the room temperature spectra show well separated resonances for the tpy protons; changing the solvent to [D_6]acetone (see below) results in overlap of the H^{A3} and H^{A6} signals. In each spectrum in Figure 13, the resonances assigned to the tpy protons reveal that pyridine rings A and D (Scheme 1) are equivalent in the NMR timescale, suggesting that there is rotation of the 4′-substituent about the C_{py}–N_{imine} bond. With the exception of proton H^{A6} in compound **3**, the only signal the line shape of which changes along the series is that assigned to H^{3B}, i.e. the proton closest to the 4′-substituent. For compound **4**, the signal is sharp at 295 K, consistent with fast rotation about the C_{py}–N_{imine} bond. Analogous dynamic behaviour is observed for the NHMe substituent in *N*-methylaniline.[46] On cooling an [D_6]acetone solution of **4**, the signal for H^{3B} splits, but only broad signals at δ 9.05 and 8.19 ppm are resolved at 195 K (Figure 14). The latter have been assigned to H^{3b} and H^{3a}, respectively (see Scheme 1) by analogy with compounds **1**–**3** (see below). For **1**, **2** and **3**, it is important to note that the solid-state structural data for these compounds reveal that the C_{py}–N_{imine} bond lengths are the same (1.38 Å). Hence, differences in the barrier to rotation about the C_{py}–N_{imine} bond are likely to be steric rather than electronic in origin. Consistent with this, we observe that on going from **2** to **3** in [D_6]DMSO, the increased steric demands of the *C*-phenyl vs. *C*-methyl substituent increases the barrier to rotation. At room temperature, the observation that H^{3B} appears as a broad signal for **1**, but a sharp singlet for **2**, indicates that introducing the *C*-methyl substituent lowers the barrier to rotation about the C_{py}–N_{imine} bond. Based on steric arguments, this was a unexpected observation. However, changing the solvent to [D_6]acetone results in the expected trend: the H^{3B} signal full-width-at-half-height 4.8, 5.3 and 9.0 Hz for **1**, **2** and **3** respectively. The solvent dependence of the dynamic behaviour of **1** can be rationalized in terms of the ability of the NH proton to engage in hydrogen bonding with a suitable acceptor.[31,47,48] DMSO is expected to be a better hydrogen-bond acceptor than acetone,[49] and association between **1** and the solvent will result in steric hindrance that will slow down the rate of rotation about C_{py}–N_{imine} bond. The hydrogen bonding capacity of the imine NH in **1** is apparent in its packing in the solid state (Figure 8), and this observation is in line with the results of several studies of phenylhydrazones which conclude that such hydrogen bonding is the predominant factor is determining solid state conformation and solution dynamic behaviour.[31,50] Consistent with the proposal that hydrogen bonding between the imine NH and solvent molecules hinders rotation about the C_{py}–N_{imine} bond is the observation that the rotation is facile in compound **4** (i.e. the *N*-methyl derivative). The ^{1}H NMR spectra of **1**, **2** and **3** at 195 K (Figure 14) are consistent with static structures in which the 4′-substituent lies in, or close to, the plane of the tpy unit. Protons H^{3a} and H^{3b} (Scheme 1) were assigned from the NOESY cross peak between H^{3a} and H^{NH}. Coupling between H^{B3a} and H^{B3b} is resolved for **1** with J = 2.1 Hz. Although each of the remaining tpy proton signals also splits at 195 K, overlap of signals precludes unambiguous assignments to rings A and D.

We consider the effects of protonation on dynamic behaviour with a detailed study of the series **1**, [H**1**]$^{+}$ and [H_2**1**]$^{2+}$. There is a significant change in the chemical shift for the signal assigned to the NH proton and signals in the aromatic region when **1** is protonated. This is exemplified by comparing the ^{1}H NMR spectra of **1** (Figure 13) and [H_2**1**][$MeOSO_3$]$_2$ (Figure 15). The figures also illustrate that in the room temperature spectrum of **1**, the signal for H^{B3} is broad while that for H^{A3} is a well-resolved doublet. In contrast, both signals are extremely broad in the spectrum of [H_2**1**][$MeOSO_3$]$_2$. Upon warming to 360 K, the resonances assigned to H^{A3} and H^{B3} sharpen (Figure 16), confirming their assignments. Low temperature ^{1}H NMR spectra of [H_2**1**][$MeOSO_3$]$_2$ could not be acquired because the compound was very poorly soluble in common low freezing point solvents. However, salts of [H**1**]$^{+}$ were more amenable to low temperature studies. Cooling an [D_6]acetone solution of [H**1**][PF_6] to 255 K results in a splitting of the signals for H^{A3} and H^{B3} to give pairs of equal intensity signals (H^{A3} δ 8.82 and 8.43 ppm, and H^{B3} δ 8.62 and 7.90 ppm). Coup-

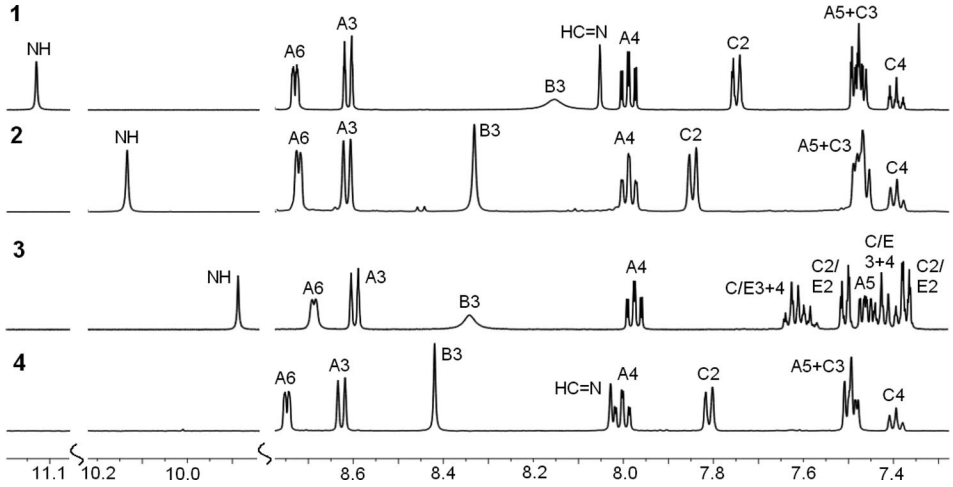

Figure 13. Aromatic and NH regions of the 500 MHz ^{1}H NMR spectra of neutral compounds **1** to **4** in [D$_6$]DMSO at 295 K. See Scheme 1 for atom labelling.

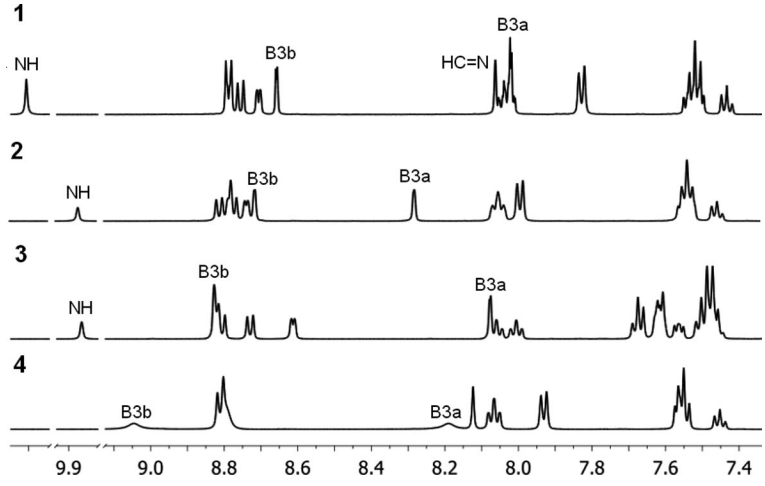

Figure 14. Aromatic and NH regions of the 500 MHz ^{1}H NMR spectra of neutral compounds **1** to **4** in [D$_6$]acetone at 195 K. See Scheme 1 for atom labelling.

ling between H^{B3a} and H^{B3b} is observed with J = 1.8 Hz. Pairs of signals for all the pyridine ring protons are resolved by 220 K. The assignments shown in the lowest trace in Figure 16 were made using NOESY and COSY experiments, starting with NOESY cross peaks between the NH_{imine} and H^{B3a}, and H^{B3a} and H^{A3} protons (see Scheme 1 for labelling). The variable temperature NMR spectroscopic data are consistent with rotation about the C_{py}–N_{imine} bond being rapid on the NMR timescale at 360 K, and frozen out at low temperatures with [H**1**]$^+$ adopting the static structure shown in Figure 5. The spectroscopic data illustrated in the figures indicate that the activation barrier to rotation increases upon protonation of **1**, and this is consistent with a greater contribution from the resonance form for [H**1**]$^+$ shown on the right of Scheme 3. Changes in the signal for H^{A3} give information concerning rotation about the C_{py}–C_{py} bonds. Again, protonation raises the energy barrier to rotation, consistent with the pyridine *N* atoms being involved in hydrogen bonding interactions with the proton. Finally, although the imine NH signal is sharp (δ 12.3 ppm at 195 K and δ 11.6 ppm at 315 K in [D$_6$]acetone) over the whole 360–195 K temperature range, the pyridinium proton is not observed above 255 K. On cooling, a broad signal at δ 13.4 ppm becomes visible at 255 K and is sharp at 195 K.

Both [H$_2$tpy]$^{2+}$ and [Htpy]$^+$ are weak acids (pK_a = 3.57 and 4.54, respectively, 298 K, in 0.2 M aqueous KCl).[51] The fact that treatment of [H$_2$**1**][MeOSO$_3$]$_2$ or [H$_2$**2**][MeOSO$_3$]$_2$ in hot MeOH with $NaBF_4$ or NH_4PF_6 results in the formation of tetrafluoroborate or hexafluorophosphate salts of [H**1**]$^+$ or [H**2**]$^+$ indicates that, in the absence of a strong hydrogen-bond acceptor (viz. [MeOSO$_3$]$^-$), [H$_2$**1**]$^{2+}$ and [H$_2$**2**]$^{2+}$ will partially deprotonate in solution. We argued that it should be possible to prepare [H$_2$**1**][PF$_6$]$_2$ by treatment of **1** with an excess of HPF_6 under conditions where **1** and [H**1**]$^+$ were the most potent proton acceptors available. The addition of HPF_6 (60% aqueous) to a solution of **1** in EtOH resulted in the immediate precipitation of a bright yellow solid. Elemental analysis was consistent with the formation of [H$_2$**1**][PF$_6$]$_2$. However, there is evidence

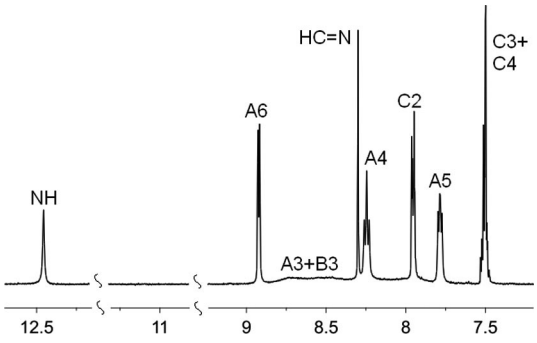

Figure 15. Aromatic and NH regions of the 500 MHz ^{1}H NMR spectra of $[H_2\mathbf{1}][MeOSO_3]_2$ in $[D_6]$DMSO at 295 K. See Scheme 1 for atom labelling.

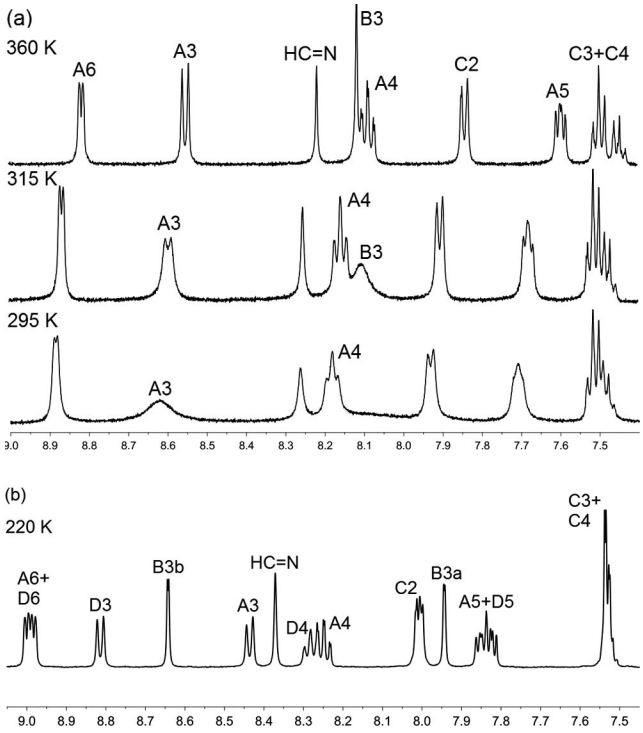

Figure 16. Aromatic region of the 500 MHz ^{1}H NMR spectra of (a) $[H_2\mathbf{1}][MeOSO_3]_2$ in $[D_6]$DMSO at 295, 315 and 360 K, and (b) $[H\mathbf{1}][PF_6]$ in $[D_6]$acetone at 220 K. See Scheme 1 for atom labelling.

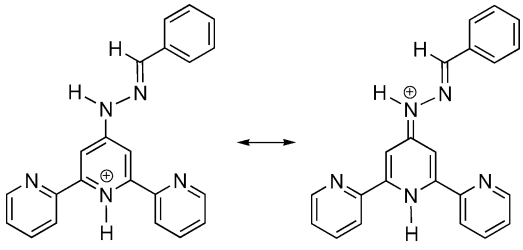

Scheme 3. Resonance structures for $[H\mathbf{1}]^+$.

that in $[D_6]$acetone solution, an equilibirium mixture of $[H_2\mathbf{1}][PF_6]_2$ and $[H\mathbf{1}][PF_6]$ exists; the ^{1}H NMR spectrum at 195 K exhibits two sets of signals (one well resolved and the other broadened).

Conclusions

We have synthesized and fully characterized four 4′-hydrazone derivatives **1**–**4** of 2,2′:6′,2′′-terpyridine which vary in their *N*- and *C*-substitution. In the solid-state structures of compounds **1**–**4**, the tpy domain adopts the anticipated *trans*,*trans*-conformation, and intramolecular steric factors compete with π-stacking effects to control the amount to which the *C*-phenyl substituent twists out of the plane of the tpy unit. In each of compounds **1** to **2**, the imine NH engages in hydrogen bonded interactions, but in **3** this appears to be unfavourable on steric grounds. In solution, variable temperature ^{1}H NMR spectroscopy shows that the increased steric demands of the *C*-phenyl in **3** vs. *C*-methyl substituent in **2** increases the barrier to rotation about the C_{py}–N_{imine} bond, while in **1**, the hydrogen bonding capabilities of the solvent to the imine NH influence this dynamic process. In **4**, rotation about the C_{py}–N_{imine} bond is facile at room temperature. Protonation of **1** results in an increase in the activation barrier to rotation, consistent with a greater π-contribution to the C_{py}–N_{imine} bond.

Experimental Section

General: ^{1}H and ^{13}C NMR spectra were recorded on a Bruker Avance DRX 500 spectrometer; the numbering scheme for the ligands is shown in Scheme 1. Chemical shifts for ^{1}H and ^{13}C NMR spectra are referenced to residual solvent peaks with respect to TMS = δ 0 ppm. Electrospray mass spectra were recorded using a Finnigan MAT LCQ mass spectrometer. Melting points were recorded on a Stuart Scientific melting point apparatus SMP3. 4′-Hydrazino-2,2′:6′,2′′-terpyridine was prepared as previously reported, and spectroscopic data were consistent with those in the literature.[25–27] In the ^{1}H NMR spectra listed below, data at 360 K are given whenever the spectrum at 295 K contains very broad or unresolved signals.

4′-(1-Methylhydrazino)-2,2′:6′,2′′-terpyridine: This was prepared as described previously, m.p. 212–214 °C (ref.[25] 217–219 °C). ^{1}H NMR spectroscopic data were consistent with literature data.[25] $^{13}C\{^1H\}$ (125 MHz, $[D_6]$DMSO, 295 K): δ = 158.2 (C^{B4}), 156.2 ($C^{A2/B2}$), 154.7 ($C^{A2/B2}$), 149.0 (C^{A6}), 137.1 (C^{A4}), 123.9 (C^{A5}), 120.7 (C^{A3}), 103.5 (C^{B3}), 41.7 (C^{Me}) ppm.

$[H_2\mathbf{1}][MeOSO_3]_2$: 4′-Hydrazino-2,2′:6′,2′′-terpyridine (0.20 g, 0.76 mmol) was dissolved in hot methanol (15 cm^3), and excess benzaldehyde (0.10 g, 0.94 mmol) was added giving a colourless solution. A few drops of concentrated H_2SO_4 were added, and a yellow precipitate formed almost immediately. The suspension was heated at reflux for 3 h and then cooled to room temperature. The bright yellow solid product was collected by filtration and washed with EtOH. $[H_2\mathbf{1}][MeOSO_3]_2$ was isolated as a yellow powder (0.42 g, 0.73 mmol, 96%). ^{1}H NMR (500 MHz, $[D_6]$DMSO, 360 K): δ = 12.02 (br., H^{NH}), 8.89 (ddd, J = 4.8, 1.7, 0.9 Hz, 2 H, H^{A6}), 8.53 (d, J = 8.0 Hz, 2 H, H^{A3}), 8.34 (s, 1 H, $H^{HC=N}$), 8.19 (td, J = 7.7, 1.7 Hz, 2 H, H^{A4}), 8.11 (s, 2 H, H^{B3}), 7.91 (dd, J = 7.9, 1.5 Hz, 2 H, H^{C2}), 7.72 (ddd, J = 7.6, 4.8, 1.0 Hz, 2 H, H^{A5}), 7.5 (m, 3 H, H^{C3+C4}), 3.39 (s, H^{OMe}, see text) ppm. ^{1}H NMR (500 MHz, $[D_6]$DMSO, 295 K): δ = 12.45 (s, NH), 8.93 (d, J = 4.4 Hz, 2 H, H^{A6}), 8.7 (v br., H^{A3}), 8.5 (v br., H^{B3}), 8.30 (s, 1 H, $H^{HC=N}$), 8.25 (t, J = 7.6 Hz, 2 H, H^{A4}), 7.96 (dd, J = 7.5, 2.0 Hz, 2 H, H^{C2}), 7.79 (dd, J = 6.8, 5.3 Hz, 2 H, H^{A5}), 7.50 (m, 3 H,

H^{C3+C4}), 3.38 (s, H^{OMe}, see text) ppm. $^{13}C\{^1H\}$ NMR (125 MHz, [D$_6$]DMSO, 295 K): δ = 156.0 (C^{B4}), 149.2 (C^{A6}), 147.8 ($C^{C=N}$), 146.8 (C^{A2+B2}), 139.8 (C^{A4}), 133.7 (C^{C1}), 130.7 (C^{C4}), 129.0 (C^{C3}), 127.8 (C^{C2}), 127.1 (C^{A5}), 122.8 (br., C^{A3}), 105 (br., H^{B3}), 53.0 (C^{Me}) ppm. ES-MS: *m*/*z* = 352 [H**1**]$^+$. $C_{24}H_{27}N_5O_9S_2$ (593.63): calcd. C 48.56, H 4.58, N 11.80; found C 48.77, H 4.21, N 11.97.

[H$_2$1][NO$_3$]$_2$: The method and scale were as for [H$_2$**1**][MeOSO$_3$]$_2$, replacing concentrated H_2SO_4 by HNO_3 (***Caution!***). [H$_2$**1**][NO$_3$]$_2$ was isolated as a bright yellow powder (0.24 g, 0.50 mmol, 70%). ^{1}H NMR (500 MHz, [D$_6$]DMSO, 295 K): δ = 12.28 (br., NH), 8.93 (d, *J* = 4.7 Hz, 2 H, H^{A6}), 8.6 (v br., H^{A3}), 8.32 (s, 1 H, $H^{HC=N}$), 8.24 (t, *J* = 7.3 Hz, 2 H, H^{A4}), 7.98 (dd, *J* = 7.8, 1.5 Hz 2 H, H^{C2}), 7.77 (dd, *J* = 7.5, 5.0 Hz, 2 H, H^{A5}), 7.50 (m, 3 H, C^{3+4}) ppm; signal for H^{B3} not observed at 295 K. $^{13}C\{^1H\}$ NMR (125 MHz, [D$_6$]DMSO, 295 K): δ = 149.1 (C^{A6}), 147.0 ($C^{C=N}$), 139.4 (C^{A4}), 133.8 (C^{C1}), 130.5 (C^{C4}), 128.9 (C^{C3}), 127.6 (C^{C2}), 126.8 (C^{A5}), 122.4 (br., C^{A3}) ppm, $C^{A2,B2,B3,B4}$ not observed . ES-MS: *m*/*z* = 352 [H**1**]$^+$. $C_{22}H_{19}N_7O_6\cdot0.25H_2O$ (401.94): calcd. C 54.83, H 4.08, N 20.34; found C 54.93, H 3.93, N 20.11.

[H$_2$1]Cl$_2$: The method and scale were as for [H$_2$**1**][MeOSO$_3$]$_2$, replacing concentrated H_2SO_4 by HCl. [H$_2$**1**]Cl$_2$ was isolated as a bright yellow powder (0.17 g, 0.40 mmol, 53%). ^{1}H NMR (500 MHz, [D$_6$]DMSO, 295 K): δ = 12.66 (s, H^{NH}), 8.93 (d, *J* = 4.3 Hz, 2 H, H^{A6}), 8.62 (br., H^{A3}), 8.37 (s, 1 H, $H^{HC=N}$), 8.24 (t, *J* = 7.6 Hz, 2 H, H^{A4}), 7.97 (d, *J* = 7.0 Hz 2 H, H^{C2}), 7.77 (dd, *J* = 6.5, 4.9 Hz, 2 H, H^{A5}), 7.51 (m, 3 H, H^{C3+4}), signal for H^{B3} not observed at 295 K ppm. $^{13}C\{^1H\}$ NMR (125 MHz, [D$_6$]DMSO, 295 K): δ = 155.6 (C^{A2+B2}), 149.1 (C^{A6}), 147.9 ($C^{C=N}$), 139.4 (C^{A4}), 133.8 (C^{C1}), 130.4 (C^{C4}), 128.9 (C^{C3}), 127.5 (C^{C2}), 126.7 (C^{C5}), 122.4 (C^{A3}), 104 (br., C^{B3}) ppm, C^{B4} not observed. ES-MS: *m*/*z* = 352 [H**1**]$^+$. $C_{22}H_{19}Cl_2N_5\cdot3.5H_2O$ (487.38): calcd. C 54.22, H 5.38, N 14.37; found C 54.02, H 5.02, N 14.40.

[H1][BF$_4$]: [H$_2$**1**][MeOSO$_3$]$_2$ (0.10 g, 0.17 mmol) was dissolved in a minimum volume of hot water and excess $NaBF_4$ was added. The yellow-green precipitate that formed was collected by filtration and washed with water and cold EtOH. [H**1**][BF$_4$] was isolated as a pale yellow solid (0.070 g, 0.16 mmol, 92%). ^{1}H NMR (500 MHz, [D$_6$]DMSO, 360 K): δ = 11.42 (br., H^{NH}), 8.82 (d, *J* = 4.8 Hz, 2 H, H^{A6}), 8.55 (d, *J* = 8.0 Hz, H^{A3}), 8.22 (s, 1 H, $H^{HC=N}$), 8.11 (s, 2 H, H^{B3}), 8.09 (t, *J* = 7.4 Hz, 2 H, H^{A4}), 7.96 (d, *J* = 6.4 Hz, 2 H, H^{C2}), 7.75 (ddd, *J* = 7.7, 4.9, 0.8 Hz, 2 H, H^{A5}), 7.5 (m, 3 H, H^{C3+4}) ppm. ^{1}H NMR (500 MHz, [D$_6$]DMSO, 295 K): δ = 12.23 (br., H^{NH}), 8.91 (d, *J* = 4.3 Hz, 2 H, H^{A6}), 8.6 (v br., $H^{A3,B3}$), 8.29 (s, 1 H, $H^{HC=N}$), 8.21 (t, *J* = 7.4 Hz, 2 H, H^{A4}), 7.96 (d, *J* = 6.4 Hz, 2 H, H^{C2}), 7.75 (t, *J* = 7.7 Hz, 2 H, H^{A5}), 7.5 (m, 3 H, H^{C3+4}) ppm. $^{13}C\{^1H\}$ NMR (125 MHz, [D$_6$]DMSO, 295 K): δ = 155.6 (C^{B4}), 149.3 (C^{A6}), 148.0 (C^{A2+B2}), 146.8 ($C^{C=N}$), 139.2 (C^{A4}), 133.8 (C^{C1}), 130.5 (C^{C4}), 128.9 (C^{C3}), 127.6 (C^{C2}), 126.8 (C^{A5}), 122.4 (br., C^{A3}), 104.1 (br., C^{B3}) ppm. ES-MS: *m*/*z* = 352 [H**1**]$^+$. $C_{22}H_{18}BF_4N_5\cdot1.5H_2O$ (466.24): calcd. C 56.67, H 4.54, N 15.02; found C 57.02, H 4.37, N 15.07.

[H1][PF$_6$]: An excess of NH_4PF_6 was added to a solution of [H$_2$**1**][MeOSO$_3$]$_2$ (0.10 g, 0.17 mmol) dissolved in a minimum volume of hot water. A pale yellow precipitate formed and was collected by fitration, washed with water and cold EtOH. [H**1**][PF$_6$] was isolated as a pale yellow solid (0.042 g, 0.084 mmol, 49%). Slow evaporation of a solution of [H**1**][PF$_6$] in acetone/water (5:1) gave X-ray-quality crystals of [H**1**][PF$_6$]·H$_2$O. ^{1}H NMR (500 MHz, [D$_6$]DMSO, 360 K): δ = 11.45 (br., H^{NH}), 8.82 (d, *J* = 4.7 Hz, 2 H, H^{A6}), 8.55 (d, *J* = 8.0 Hz, H^{A3}), 8.22 (s, 1 H, $H^{HC=N}$), 8.11 (s, 2 H, H^{B3}), 8.09 (dt, *J* = 7.8, 1.7 Hz, 2 H, H^{A4}), 7.84 (d, *J* = 7.0 Hz, 2 H, H^{C2}), 7.75 (dd, *J* = 7.5, 4.7 Hz, 2 H, H^{A5}), 7.50 (m, 3 H, H^{C3+4}) ppm. ^{1}H NMR (500 MHz, [D$_6$]DMSO, 295 K): δ = 11.97 (s, H^{NH}), 8.68 (d, *J* = 4.0 Hz, 2 H, H^{A6}), 8.62 (br., H^{A3}), 8.25 (s, 1 H, $H^{HC=N}$), 8.16 (t, *J* = 7.4 Hz, 2 H, H^{A4}), 8.1 (v br., H^{B3}), 7.92 (d, *J* = 7.1 Hz, 2 H, H^{C2}), 7.69 (t, *J* = 5.2 Hz, 2 H, H^{A5}), 7.50 (m, 3 H, H^{C3+4}) ppm. $^{13}C\{^1H\}$ NMR (125 MHz, [D$_6$]DMSO, 295 K): δ = 155.4 (C^{B4}), 149.4 (C^{A6}), 148.5 (C^{A2+B2}), 146.6 ($C^{C=N}$), 139.1 (C^{A4}), 133.9 (C^{C1}), 130.4 (C^{C4}), 128.9 (C^{C3}), 127.5 (C^{C2}), 126.6 (C^{A5}), 122.4 (br., C^{A3}), 104.2 (br., C^{B3}) ppm. ES-MS: *m*/*z* = 352 [H**1**]$^+$. $C_{22}H_{18}F_6F_6N_5P\cdot0.75H_2O$ (624.88): calcd. C 51.72, H 3.85, N 13.71; found C 51.71, H 3.86, N 13.63.

1: [H$_2$**1**][MeOSO$_3$]$_2$ (0.50 g, 0.87 mmol) was dissolved in water (100 cm^3) to give a yellow solution. Solid K_2CO_3 was added until a colourless solution was obtained. The solution became almost colourless and was extracted into CH_2Cl_2 (3 × 50 cm^3) and the solution was dried with Na_2SO_4. Solvent was removed to give neutral **1** which was purified by chromatography using a short column (alumina, CH_2Cl_2 with 1% MeOH). **1** was isolated as a white solid (0.25 g, 0.71 mmol, 82%); m.p. 210–212 °C. ^{1}H NMR (500 MHz, [D$_6$]DMSO, 295 K): δ = 11.14 (H^{NH}), 8.74 (ddd, *J* = 4.7, 1.7, 0.8 Hz, 2 H, H^{A6}), 8.62 (td, *J* = 8.0, 1.0 Hz, 2 H, H^{A3}), 8.16 (br., H^{B3}), 8.06 (s, 1 H, $H^{HC=N}$), 7.99 (td, *J* = 7.6, 1.8 Hz, 2 H, H^{A4}), 7.76 (dd, *J* = 7.2, 1.3 Hz, 2 H, H^{C2}), 7.48 (m, 4 H, H^{A5+C3}), 7.39 (tt, *J* = 7.3, 1.3 Hz, 1 H, H^{C4}) ppm. $^{13}C\{^1H\}$ NMR (125 MHz, [D$_6$]DMSO, 295 K): δ = 155.5, ($C^{A2/B2}$), 155.4 ($C^{A2/B2}$), 152.7 (C^{B4}), 149.2 (C^{A6}), 140.7 ($C^{C=N}$), 137.2 (C^{A4}), 134.8 (C^{C1}), 129.1 (C^{C4}), 128.9 (C^{C3}), 126.3 (C^{C2}), 124.2 (C^{A5}), 120.8 (C^{A3}), 103.8 (br., C^{B3}) ppm. ES-MS: *m*/*z* = 352 [H**1**]$^+$. $C_{22}H_{17}N_5\cdot H_2O$ (369.42): calcd. C 71.53, H 5.18, N 18.96; found C 71.62, H 4.97, N 18.88.

[H$_2$1][PF$_6$]$_2$: HPF_6 (60% in water, 2 cm^3) was added to a solution of **1** (0.10 g, 0.28 mmol) in EtOH (30 cm^3). A bright yellow precipitate which formed was collected by fitration and washed with EtOH (10 cm^3). The solid was dissolved in acetone, HPF_6 (1 cm^3) was added and the solution was filtered to remove a small amount of solid material. Et_2O was added and the resulting yellow precipitate was collected. [H$_2$**1**][PF$_6$]$_2$ (0.036 g, 0.056 mmol, 20%). ^{1}H NMR (500 MHz, [D$_6$]DMSO, 360 K): δ = 11.74 (s, H^{NH}), 8.86 (d, *J* = 4.7 Hz, 2 H, H^{A6}), 8.54 (d, *J* = 7.9 Hz, H^{A3}), 8.28 (s, 1 H, $H^{HC=N}$), 8.15 (dt, *J* = 7.9, 1.6 Hz, 2 H, H^{A4}), 8.10 (s, 2 H, H^{B3}), 7.89 (d, *J* = 6.9 Hz, 2 H, H^{C2}), 7.67 (dd, *J* = 7.1, 5.2 Hz, 2 H, H^{A5}), 7.49 (m, 3 H, H^{C3+4}) ppm. ^{1}H NMR (500 MHz, [D$_6$]DMSO, 295 K): δ = 12.25 (s, H^{NH}), 8.92 (d, *J* = 4.4 Hz, 2 H, H^{A6}), 8.62 (br., H^{A3}), 8.31 (s, 1 H, $H^{HC=N}$), 8.23 (t, *J* = 7.7 Hz, 2 H, H^{A4}), 8.10 (v br., H^{B3}), 7.97 (d, *J* = 6.9 Hz, 2 H, H^{C2}), 7.76 (dd, *J* = 6.8, 5.1 Hz, 2 H, H^{A5}), 7.52 (m, 3 H, H^{C3+4}) ppm. $^{13}C\{^1H\}$ NMR (125 MHz, [D$_6$]DMSO, 295 K): δ = 155.8 (C^{A2+B2}), 149.2 (C^{A6}), 147.3 ($C^{C=N}$), 139.5 (C^{A4}), 133.7 (C^{C1}), 130.6 (C^{C4}), 128.9 (C^{C3}), 127.7 (C^{C2}), 126.9 (C^{A5}) ppm, $C^{A3,B3,B4}$ not observed. ES-MS: *m*/*z* = 352 [H**1**]$^+$. $C_{22}H_{18}F_{12}N_5P_2\cdot1.5H_2O$ (669.36): calcd. C 39.42, H 3.31, N 10.45; found C 39.69, H 3.26, N 10.14.

[H$_2$2][MeOSO$_3$]$_2$: 4′-Hydrazino-2,2′:6′,2′′-terpyridine (0.20 g, 0.76 mmol) was dissolved in hot methanol (15 cm^3), and excess acetophenone (0.10 g, 0.83 mmol) was added giving a colourless solution. A few drops of concentrated H_2SO_4 were added, and a bright yellow precipitate formed after heating the mixture for a few minutes. The suspension was heated at reflux for 3 h and then cooled to room temperature. The bright yellow solid was collected by filtration and washed well with MeOH. [H$_2$**2**][MeOSO$_3$]$_2$ was isolated as a yellow powder (0.45 g, 0.76 mmol, 100%). ^{1}H NMR (500 MHz, [D$_6$]DMSO, 360 K): δ = 11.28 (s, H^{NH}), 8.93 (d, *J* = 4.4 Hz, 2 H, H^{A6}), 8.57 (br., H^{A3}), 8.28 (s, 2 H, H^{B3}), 8.25 (t, *J* = 7.7 Hz, 2 H, H^{A4}), 8.04 (dd, *J* = 7.7, 1.4 Hz, 2 H, H^{C2}), 7.78 (dd, *J* = 6.8, 5.2 Hz, 2 H, H^{A5}), 7.50 (m, 3 H, C^{3+4}), 3.38 (s, H^{OMe}, see

text), 2.50 (H^{CMe}, overlaps with solvent peak) ppm. $^{13}C\{^1H\}$ NMR (125 MHz, [D_6]DMSO, 295 K): δ = 149.2 (C^{A6}), 139.5 (C^{A4}), 128.5 ($C^{C3,C4}$), 126.8 (C^{A5}), 126.5 (C^{C2}), 14.4 (C^{MeC}) ppm, $C^{A2,A3,B2,B3,B4,C1,C=N}$ not observed. ES-MS: *m*/*z* = 366 [H**2**]$^+$. $C_{25}H_{27}N_5O_8S_2{\cdot}0.75H_2O$ (603.15): calcd. C 49.78, H 4.76, N 11.61; found , C 49.72, H 4.61, N 11.41.

[H2][BF$_4$]: [H_2**2**][$MeOSO_3$]$_2$ (0.10 g, 0.17 mmol) was dissolved in a minimum volume of hot water and an excess of $NaBF_4$ was added. The mixture was heated to 50 °C and was maintained at this temperature with stirring for 1 h, after which time a yellow-green solid had formed. The precipitate was collected by filtration and was washed well with water and cold EtOH. [H**2**][BF_4] was isolated as a yellow-green solid (0.062 g, 0.13 mmol, 80%). ^1H NMR (500 MHz, [D_6]DMSO, 360 K): δ = 10.67 (br., H^{NH}), 8.81 (ddd, *J* = 4.3, 1.7, 0.9 Hz, 2 H, H^{A6}), 8.46 (dt, *J* = 8.0, 1.0 Hz, 2 H, H^{A3}), 8.22 (s, 2 H, H^{B3}), 8.09 (dt, *J* = 8.0, 1.7 Hz, 2 H, H^{A4}), 7.91 (dd, *J* = 8.3, 1.4 Hz, 2 H, H^{C2}), 7.61 (ddd, *J* = 7.6, 4.8, 1.1 Hz, 2 H, H^{A5}), 7.44 (m, 3 H, H^{C3+4}), 2.47 (C^{Me}) ppm. $^{13}C\{^1H\}$ NMR (125 MHz, [D_6]DMSO, 295 K): δ = 149.3 (C^{A6}), 139.2 (C^{A4}), 137.6 (C^{C1}), 129.6 (C^{C4}), 128.6 (C^{C3}), 126.6 (C^{C2}), 126.4 (C^{A5}), 122.3 (C^{A3}), 104.5 (br., C^{B3}), 14.3 (C^{Me}) ppm, C $^{B4,A2,B2,C=N}$ not observed. ES-MS: *m*/*z* = 366 [H**2**]$^+$. $C_{23}H_{20}BF_4N_5{\cdot}0.5H_2O$ (462.25): calcd. C 59.76, H 4.58, N 15.15; found C 59.93, H 4.41, N 15.17.

2: [H_2**2**][$MeOSO_3$]$_2$ (0.30 g, 0.51 mmol) was dissolved in warm H_2O (10 cm^3) and the mixture was filtered through fluted filter paper to remove a small amount of solid impurities. Solid K_2CO_3 was added to the cream precipitate that formed was extracted into CH_2Cl_2 (3 × 100 cm^3) and dried with Na_2SO_4. Removal of the solvent gave **2** which was purified by chromatography using a short column (alumina, CH_2Cl_2 with 1% MeOH). **2** was isolated as an off-white solid (0.11 g, 0.30 mmol, 58%); m.p. 192–193 °C. ^1H NMR (500 MHz, [D_6]DMSO, 295 K): δ = 10.13 (s, H^{NH}), 8.72 (d, *J* = 4.1 Hz, 2 H, H^{A6}), 8.61 (d, *J* = 7.9 Hz, 2 H, H^{A3}), 8.33 (s, 2 H, H^{B3}), 7.99 (t, *J* = 7.6 Hz, 2 H, H^{A4}), 7.85 (d, *J* = 7.3 Hz, 2 H, H^{C2}), 7.47 (m, 4 H, H^{C3+A5}), 7.39 (m, 1 H, H^{C4}), 2.37 (s, 3 H, H^{Me}) ppm. $^{13}C\{^1H\}$ NMR (125 MHz, [D_6]DMSO, 295 K): δ = 155.7, (C^{A2+B2}), 153.5 (C^{B4}), 149.1 (C^{A6}), 145.1 ($C^{C=N}$), 138.8 (C^{C1}), 137.2 (C^{A4}), 128.5 (C^{C3}), 128.4 (C^{C4}), 125.7 (C^{C2}), 124.1 (C^{A5}), 120.7 (C^{A3}), 104.3 (br., C^{B3}), 13.6 (C^{Me}) ppm. ES-MS: *m*/*z* = 366 [H**2**]$^+$. $C_{23}H_{19}N_5{\cdot}0.33H_2O$ (371.38): calcd. C 74.38, H 5.34, N 18.86; found C 74.58, H 5.37, N 18.72.

[$H_2$3][$MeOSO_3$]$_2$: Excess benzophenone (0.16 g, 0.87 mmol) and 4′-hydrazino-2,2′:6′,2′′-terpyridine (0.20 g, 0.76 mmol) were dissolved in hot MeOH (20 cm^3). A few drops of concentrated H_2SO_4 were added to the solution and a white precipitate formed which redissolved on heating. The solution was heated at reflux for 3 h to ensure that the reaction had reached completion. On cooling the reaction mixture to room temperature, only a small amount of solid precipitated. Et_2O was added to afford [H_2**3**][$MeOSO_3$]$_2$ as a bright yellow powder which was collected and washed with MeOH (0.42 g, 0.64 mmol, 85%). ^1H NMR (500 MHz, [D_6]DMSO, 295 K): δ = 10.74 (s, 1 H, NH), 8.92 (d, *J* = 3.8 Hz, 2 H, H^{A6}), 8.6 (v br., 2 H, H^{A3}), 8.33 (br., 2 H, H^{B3}), 8.24 (br.dd, *J* = 7.8, 4.6 Hz, 2 H, H^{A4}), 7.77 (br.dd, *J* = 5.7, 4.0 Hz, 2 H, H^{A5}), 7.67 (m, 5 H, $H^{C/E}$), 7.46 (m, 5 H, $H^{C/E}$), 3.37 (s, 6 H, H^{Me}) ppm. ^1H NMR ([D_6]-DMSO, 360 K): δ = 10.20 (s, NH), 8.84 (d, *J* = 4.7 Hz, 2 H, H^{A6}), 8.48 (d, *J* = 7.9 Hz, 2 H, H^{A3}), 8.30 (s, 2 H, H^{B3}), 8.13 (td, *J* = 7.8, 1.6 Hz, 2 H, H^{A4}), 7.66 (m, 7 H, $H^{A5+C/E}$), 7.45 (m, 3 H, $H^{C/E}$), 7.42 (dd, *J* = 7.8. 1.5 Hz, 2 H, $H^{C/E}$) ppm. $^{13}C\{^1H\}$ NMR ([D_6]-DMSO, 295 K): δ = 149.1 (C^{A6}), 139.1 (C^{A4}), 126.7 (C^{A5}), 132.3 ($C^{C/E1}$), 137.1 ($C^{C/E1}$), 130.0 ($C^{C/E}$), 129.6 ($C^{C/E}$), 129.0 ($C^{C/E}$), 128.6 ($C^{C/E}$), 127.7 ($C^{C/E}$), 52.8 (C^{Me}) ppm, $C^{A2,A3,B2,B3,B4,C=N}$ not observed. ES-MS: *m*/*z* = 428 [H**3**]$^+$. $C_{30}H_{29}N_5O_8S_2{\cdot}2H_2O$ (687.74): calcd. C 52.39, H 4.84, N 10.18; found C 52.28, H 4.67, N 10.22.

[H3][BF$_4$]: [H_2**3**][$MeOSO_3$]$_2$ (0.20 g, 0.31 mmol) was dissolved in hot water (10 cm^3) and excess $NaBF_4$ was added. After stirring at room temperature for 1 h, the resulting solid was collected and washed well with water and cold EtOH. [H**3**][BF_4] was isolated as a green-yellow powder (0.06 g, 0.12 mmol, 37%). ^1H NMR ([D_6]-DMSO, 295 K): δ = 10.53 (s, 1 H, NH), 8.86 (br.d, *J* = 3.3 Hz, 2 H, H^{A6}), 8.53 (br. s, 2 H, H^{A3}), 8.33 (br. s, 2 H, H^{B3}), 8.17 (t, *J* = 7.1 Hz, 2 H, H^{A4}), 7.66 (m, 7 H, $H^{A5+C/E}$), 7.46 (dq, *J* = 4.9, 1.7 Hz, 3 H, $H^{C/E}$), 7.45 (d, *J* = 3.3 Hz, 2 H, H^{C2}) ppm. $^{13}C\{^1H\}$ NMR ([D_6]DMSO, 295 K): δ = 149.2 (C^{A6}), 138.8 (C^{A4}), 137.4 ($C^{C1/E1}$), 132.4 ($C^{C1/E1}$), 129.8 ($C^{C4/E4}$), 129.7 ($C^{C4/E4}$), 129.5 ($C^{C/E2/3}$), 129.0 ($C^{C/E2/3}$), 128.6 ($C^{C/E2/3}$), 127.4 ($C^{C/E2/3}$), 126.1 (C^{A5}), 122.0 (H^{A3}), 105.4 (H^{B3}) ppm, $C^{A2,B2,B4,C=N}$ not observed. ES-MS: *m*/*z* = 428 [H**3**]$^+$. $C_{28}H_{22}BF_4N_5{\cdot}H_2O$ (533.33): calcd. C 63.06, H 4.54, N 13.13; found C 62.86, H 4.16, N 12.93.

3: [H_2**3**][$MeOSO_3$]$_2$ (0.25 g, 0.38 mmol) was dissolved in H_2O (10 cm^3), and solid K_2CO_3 (5 g) was added. CH_2Cl_2 (50 cm^3) was added and the biphasic mixture was sonicated for 1 h. The two phases were separated and the aqueous layer extracted with CH_2Cl_2 (3 × 300 cm^3). The combined organic fractions were dried with Na_2SO_4 and the solvent was removed to give **3** as a pale orange microcrystalline solid which was recrystallised from EtOH/CH_2Cl_2 to give **3** as an off-white solid (0.065 g, 0.15 mmol, 40%); m.p. 212–214 °C. ^1H NMR ([D_6]DMSO, 295 K): δ = : 9.89 (s, NH), 8.69 (d, *J* = 3.9 Hz, H^{A6}), 8.60 (d, *J* = 7.9 Hz, H^{A3}), 8.34 (s, H^{B3}), 7.97 (td, *J* = 7.7, 1.7 Hz, H^{A4}), 7.61 (m, 3 H, $H^{C/E3+4}$), 7.51 (dd, *J* = 8.3, 1.4 Hz, 2 H, $H^{C2/E2}$), 7.46 (ddd, *J* = 7.4, 4.7, 1.1 Hz, H^{A5}), 7.41 (m, 3 H, $H^{C/E3+4}$), 7.37 (dd, *J* = 8.0, 1.5 Hz, 2 H, $H^{C2/E2}$) ppm. $^{13}C\{^1H\}$ ([D_6]DMSO, 295 K) δ /ppm 155.7 ($C^{A2/B2}$), 155.3 ($C^{A2/B2}$), 153.1 (C^{B4}), 149.1 (C^{A6}), 147.3 (C=N), 138.3 ($C^{C1/E1}$), 137.1 (C^{A4}), 133.0 ($C^{C1/E1}$), 129.4 ($C^{C3/E3}$), 129.2 ($C^{C4/E4}$), 129.1 ($C^{C3/E3}$), 128.6 ($C^{C4/E4}$), 128.5 ($C^{C3/E3}$), 126.6 ($C^{C2/E2}$), 124.1 (C^{A5}), 120.7 (C^{A3}), 105.0 (C^{B3}). ES-MS: *m*/*z* = 428 [H**3**]$^+$. $C_{28}H_{21}N_5{\cdot}0.5H_2O$ (436.51): calcd. C 77.04, H 5.08, N 16.04; found C 76.75, H 4.97, N 16.05.

[$H_2$4][$MeOSO_3$]$_2$: Excess benzaldehyde (0.10 g, 0.94 mmol) was added to a solution of 4′-(1-methylhydrazino)-2,2′:6′,2′′-terpyridine (0.20 g, 0.72 mmol) in hot methanol(15 cm^3). Upon the addition of a few drops of concentrated H_2SO_4 followed by stirring for a few minutes, the cloudy reaction mixture converted into a pale yellow solution. This was heated under reflux for 12 h, after which time it was cooled to room temperature. Et_2O was added until a cream precipitate began to form.The reaction mixture was left in the freezer overnight and was then filtered. The solid residue was washed well with Et_2O, and [H_2**4**][$MeOSO_3$]$_2$ was isolated as a pale yellow microcrystalline solid (0.33 g, 0.56 mmol, 78%). ^1H NMR (500 MHz, [D_6]DMSO, 295 K): δ = 8.94 (d, *J* 4.6 Hz, 2 H, H^{A6}), 8.81 (d, *J* 8.0 Hz, 2 H, H^{A3}), 8.46 (s, 2 H, H^{B3}), 8.37 (s, 1 H, $H^{HC=N}$), 8.24 (t, *J* 7.5 Hz, 2 H, H^{A4}), 8.00 (d, *J* 7.2 Hz, 2 H, H^{C2}), 7.80 (dd, *J* 7.2, 5.2 Hz, 2 H, H^{A5}), 7.54 (m, 2 H, $H^{C3,C4}$), 3.83 (s, 3 H, H^{Me}), 3.37 (s, H^{OMe}, see text) ppm. $^{13}C\{^1H\}$ NMR (125 MHz, [D_6]DMSO, 295 K): δ = 157.1 (C^{B4}), 147.7 ($C^{A2,B2}$), 149.0 (C^{A6}), 144.1 ($C^{C=N}$), 139.3 (C^{A4}), 134.5 (C^{C1}), 130.3 (C^{C4}), 129.0 (C^{C3}), 126.9 (C^{C2}), 126.4 (C^{A5}), 122.5 (C^{A3}), 105.8 (C^{B3}), 52.8 (C^{OMe}), 33.3 (C^{Me}) ppm. ES-MS: *m*/*z* = 366 [H**4**]$^+$. $C_{25}H_{27}N_5O_8S_2{\cdot}H_2O$ (607.66): calcd. C 49.41, H 4.81, N 11.53; found C 49.37, H 4.55, N 11.66.

[H4][BF$_4$]: [H_2**4**][$MeOSO_3$]$_2$ (0.15 g, 0.26 mmol) was dissolved in a hot 1: 4 MeOH/H_2O (50 cm^3) mixture and excess aqueous solution of $NaBF_4$ was added to give a pale yellow precipitate which was collected and washed well with water and a little MeOH (0.096 g,

0.21 mmol, 83%). ^{1}H NMR (500 MHz, [D$_6$]DMSO, 295 K): δ = 8.90 (d, J = 4.4 Hz, 2 H, H^{A6}), 8.76 (d, J = 8.2 Hz, 2 H, H^{A3}), 8.45 (s, 2 H, H^{B3}), 8.30 (s, 1 H, H$^{HC=N}$), 8.21 (t, J = 7.4 Hz, 2 H, H^{A4}), 7.96 (d, J = 7.3 Hz, 2 H, H^{C2}), 7.72 (dd, J = 7.0, 5.0 Hz, 2 H, H^{A5}), 7.54 (t, J = 7.4 Hz, 2 H, H^{C3}), 7.48 (t, J = 7.3 Hz, H^{C4}), 3.78 (s, 3 H, H^{Me}) ppm. ^{13}C{^{1}H} NMR (125 MHz, [D$_6$]DMSO, 295 K): δ = 149.1 (C^{A6}), 145.5 (C$^{C=N}$), 138.9 (C^{A4}), 130.0 (C^{C4}), 129.0 (C^{C3}), 127.5 (C^{C2}), 126.2 (C^{A5}), 122.3 (C^{A3}), 105.7 (C^{B3}), 39.5 (C^{Me}) ppm, C^{A2,B2,B4,C1} not observed. ES-MS: m/z = 366 [**H4**]$^+$, 388 [**4** + Na]$^+$, 753 [2(**4**) + Na]$^+$. $C_{23}H_{20}BF_4N_5 \cdot 0.75H_2O$ (466.76): calcd. C 59.18, H 4.64, N 15.00; found C 59.27, H 4.33, N 14.92.

4: [H$_2$**4**][MeOSO$_3$]$_2$ (0.10 g, 0.17 mmol) was dissolved in H_2O (10 cm^3) and solid K_2CO_3 was added until a preciptate formed. The cream solid was extracted into CH_2Cl_2 (3 × 30 cm^3), the combined extracts were dried with $MgSO_4$ and the solvent was removed. The residue was recrystallised from CH_2Cl_2/EtOH (with added solid K_2CO_3 to ensure complete deprotonation). Compound **4** was isolated as a cream microcrystalline solid (0.015 g, 0.041 mmol, 24%); m.p. 211–212 °C. ^{1}H NMR (500 MHz, [D$_6$]DMSO, 295 K): δ = 8.75 (ddd, J = 4.8, 1.6, 0.8 Hz, 2 H, H^{A6}), 8.63 (d, J = 7.9 Hz, 2 H, H^{A3}), 8.42 (s, 2 H, H^{B3}), 8.03 (s, 1 H, H$^{HC=N}$), 8.00 (td, J = 7.8, 1.8 Hz, 2 H, H^{A4}), 7.81 (d, J = 7.3 Hz, 2 H, H^{C2}), 7.49 (m, 4 H, H^{C3+A5}), 7.40 (t, J = 7.3 Hz, 1 H, H^{C4}), 3.60 (s, 3 H, H^{Me}) ppm. ^{13}C{^{1}H} NMR (125 MHz, [D$_6$]DMSO, 295 K): δ = 155.7 (C$^{A2/B2}$), 155.6 (C$^{A2/B2}$), 154.6 (C^{B4}), 149.3 (C^{A6}), 139.4 (C^{A4}), 137.4 (C$^{C=N}$), 135.8 (C^{C1}), 129.0 (C^{C3+C4}), 126.6 (C^{C2}), 124.4 (C^{A5}), 121.1 (C^{A3}), 105.4 (C^{B3}), 32.8 (C^{Me}) ppm. ES-MS: m/z = 366 [**H4**]$^+$. $C_{23}H_{19}N_5 \cdot H_2O$ (383.45): calcd. C 72.04, H 5.52, N 18.26; found C 72.00, H 5.25, N 18.07.

Crystal Structure Determinations. General: Data were collected on a Bruker–Nonius Kappa or Stoe IPDS CCD instrument; data reduction, solution and refinement used the programs COLLECT[52] and SIR92[53] or XRED[54] and SHELXS86,[55] DENZO/SCALEPACK[56] and CRYSTALS.[57] Structures have been analysed using Mercury v. 1.4.2,[58] and searches for related structures carried out in the Cambridge Structural Database (v. 5.28)[59] using Conquest v. 1.9.[58]

Crystal Data for 1: $C_{22}H_{17}N_5$, M = 351.41, monoclinic, space group $C2/c$, a = 14.0879(8), b = 12.5006(6), c = 20.1787(9) Å, β = 94.112(3)°, U = 3544.5(3) Å^3, Z = 8, D_c = 1.317 Mg m^{-3}, μ(Mo-K_α) = 0.082 mm^{-1}, T = 173 K, 4058 reflections collected. Refinement of 2306 reflections (244 parameters) with $I > 2.0\sigma$ (I) converged at final $R1$ = 0.0394 [$R1$ (all data) = 0.0845], $wR2$ = 0.0428 [$wR2$ (all data) = 0.0782], gof = 0.919.

Crystal Data for [H1][PF$_6$]·H$_2$O: $C_{22}H_{20}F_6N_5O_1P_1$, M = 515.40, triclinic, space group $P\bar{1}$, a = 8.5007(7), b = 11.4295(7), c = 12.079(1) Å, α = 75.730(5), β = 89.492(4), γ = 85.558(5)°, U = 1133.9(2) Å^3, Z = 2, D_c = 1.509 Mg m^{-3}, μ(Mo-K_α) = 0.197 mm^{-1}, T = 173 K, 5171 reflections collected. Refinement of 2616 reflections (316 parameters) with $I > 1.0\sigma$ (I) converged at final $R1$ = 0.0955 ($R1$ (all data) = 0.1851), $wR2$ = 0.0898 [$wR2$ (all data) = 0.1395], gof = 1.020.

Crystal Data for [H$_2$1]Cl$_2$·DMSO: $C_{24}H_{25}Cl_2N_5O_1S_1$, M = 502.47, triclinic, space group $P\bar{1}$, a = 7.228(1), b = 13.115(3), c = 13.320(3) Å, α = 77.47(3), β = 74.47(3), γ = 86.72(3)°, U = 1187.7(5) Å^3, Z = 2, D_c = 1.405 Mg m^{-3}, μ(Mo-K_α) = 0.389 mm^{-1}, T = 173 K, 10344 reflections collected. Refinement of 6375 reflections (298 parameters) with $I > 2.0\sigma$ (I) converged at final $R1$ = 0.0528 [$R1$ (all data) = 0.0826], $wR2$ = 0.0491 [$wR2$ (all data) = 0.0618], gof = 1.079.

Crystal Data for [H2][BF$_4$]: $C_{23}H_{20}BF_4N_5$, M = 453.25, monoclinic, space group $C2/c$, a = 21.8489(2), b = 13.7414(1), c = 14.6131(2) Å, β = 98.8945(5)°, U = 4334.60(8) Å^3, Z = 8, D_c = 1.389 Mg m^{-3}, μ(Mo-K_α) = 0.108 mm^{-1}, T = 173 K, 6359 reflections collected. Refinement of 3549 reflections (335 parameters) with $I > 3.0\sigma$ (I) converged at final $R1$ = 0.0530 [$R1$ (all data) = 0.0821], $wR2$ = 0.0511 [$wR2$ (all data) = 0.0630], gof = 1.297.

Crystal Data for [H$_2$2][NO$_3$][MeOSO$_3$]·H$_2$O: $C_{24}H_{26}N_6O_8S$, M = 588.57, monoclinic, space group $P2_1/c$, a = 8.3471(4), b = 27.284(1), c = 11.7194(4) Å, β = 106.504(3)°, U = 2559.0(2) Å^3, Z = 4, D_c = 1.450 Mg m^{-3}, μ(Mo-K_α) = 0.188 mm^{-1}, T = 173 K, 5797 reflections collected. Refinement of 3348 reflections (352 parameters) with $I > 1.0\sigma$ (I) converged at final $R1$ = 0.0690 [$R1$ (all data) = 0.1279], $wR2$ = 0.0671 [$wR2$ (all data) = 0.0944], gof = 1.125.

Crystal Data for 2: $C_{23}H_{19}N_5$, M = 365.44, monoclinic, space group $P2_1/n$, a = 16.547(1), b = 5.4934(4), c = 20.324(1) Å, β = 99.378(3)°, U = 1822.8(2) Å^3, Z = 4, D_c = 1.332 Mg m^{-3}, μ(Mo-K_α) = 0.082 mm^{-1}, T = 173 K, 3887 reflections collected. Refinement of 2614 reflections (253 parameters) with $I > 1.0\sigma$ (I) converged at final $R1$ = 0.0447 [$R1$ (all data) = 0.0752], $wR2$ = 0.0523 [$wR2$ (all data) = 0.0714], gof = 1.139.

Crystal Data for [H3][MeOSO$_3$]: $C_{29}H_{25}N_5O_4S$, M = 539.61, monoclinic, space group $P2_1/c$, a = 8.9734(3), b = 23.860(1), c = 12.3514(3) Å, β = 105.356(2)°, U = 2550.1(2) Å^3, Z = 4, D_c = 1.405 Mg m^{-3}, μ(Mo-K_α) = 0.174 mm^{-1}, T = 173 K, 5813 reflections collected. Refinement of 3582 reflections (352 parameters) with $I > 1.7\sigma$ (I) converged at final $R1$ = 0.0495 [$R1$ (all data) = 0.0873], $wR2$ = 0.0543 [$wR2$ (all data) = 0.0684], gof = 1.150.

Crystal Data for 3·CH$_2$Cl$_2$: $C_{29}H_{23}Cl_2N_5$, M = 512.44, monoclinic, space group $P2_1/c$, a = 10.8031(4), b = 9.6855(4), c = 24.417(1) Å, β = 99.785(2)°, U = 2517(2) Å^3, Z = 4, D_c = 1.352 Mg m^{-3}, μ(Mo-K_α) = 0.286 mm^{-1}, T = 173 K, 4905 reflections collected. Refinement of 3632 reflections (325 parameters) with $I > 3.0\sigma$ (I) converged at final $R1$ = 0.0379 [$R1$ (all data) = 0.0507], $wR2$ = 0.0441 [$wR2$ (all data) = 0.0554], gof = 1.111.

Crystal Data for 4: $C_{23}H_{19}N_5$, M = 365.44, monoclinic, space group $P2_1/n$, a = 13.7297(8), b = 8.5408(5), c = 15.9176(9) Å, β = 102.628(4)°, U = 1821.4(2) Å^3, Z = 4, D_c = 1.333 Mg m^{-3}, μ(Mo-K_α) = 0.082 mm^{-1}, T = 173 K, 4369 reflections collected. Refinement of 2626 reflections (253 parameters) with $I > 1.5\sigma$ (I) converged at final $R1$ = 0.0454 [$R1$ (all data) = 0.0851], $wR2$ = 0.0562 [$wR2$ (all data) = 0.0760], gof = 1.110.

CCDC-681421 (for [H$_2$**1**]Cl$_2$·DMSO), -681422 (for [H$_2$**2**][NO$_3$]-[MeOSO$_3$]·H$_2$O), -681423 (for [H**1**][PF$_6$]·H$_2$O), -681424 (for [H**2**][BF$_4$]), -681425 (for [H**3**][MeOSO$_3$]), -681426 (for **1**), -681427 (for **2**), -681428 (for **3**·CH$_2$Cl$_2$) and -681429 (for **4**) contain the supplementary crystallographic data for this paper. These data can be obtained free of charge from The Cambridge Crystallographic Data Centre via www.ccdc.cam.ac.uk/data_request/cif.

Supporting Information (see footnote on the first page of this article): Table S1 (hydrogen-bonded interactions in [H$_2$**2**][NO$_3$]-[MeOSO$_3$]·H$_2$O); Figure S1 (packing of [H$_2$**2**]$^{2+}$ cations in [H$_2$**2**][NO$_3$][MeOSO$_3$]·H$_2$O); Figure S2 (packing of [H**1**]$^+$ cations in [H**1**][PF$_6$]·H$_2$O); Figure S3 packing of [H**2**]$^+$ cations and association with BF$_4^-$ anions in [H**2**][BF$_4$].

Acknowledgments

We thank the Swiss National Science Foundation and the University of Basel for financial support.

[1] C. Serbutoviez, C. Bosshard, G. Knöpfle, P. Wyss, P. Prêtre, P. Günter, K. Schenk, E. Solari, G. Chapuis, *Chem. Mater.* **1995**, *7*, 1198–1206.
[2] D. Lupo, H. Ringsdorf, A. Schuster, M. Seitz, *J. Am. Chem. Soc.* **1994**, *116*, 10498–10506.
[3] D. Saravanakumar, S. Devaraj, S. Iyyampillai, K. Mohandoss, M. Kandaswamy, *Tetrahedron Lett.* **2008**, *49*, 127–132.
[4] D. Millán, M. Domínguez, M. C. Rezende, *Dyes Pigm.* **2008**, *77*, 441–445.
[5] R. S. Becker, F. Chagneau, *J. Am. Chem. Soc.* **1992**, *114*, 1373–1381.
[6] V. Getautis, J. V. Grazulevicius, M. Daskeviciene, T. Malinauskas, V. Jankauskas, J. Sidaravicius, A. Undzenas, *Eur. Polym. J.* **2007**, *43*, 3597–3603.
[7] C. A. M. Fraga, E. J. Barreiro, *Curr. Med. Chem.* **2006**, *13*, 167–198.
[8] S. Rollas, S. G. Küçükgüzel, *Molecules* **2007**, *12*, 1910–1939.
[9] C. M. Armstrong, P. V. Bernhardt, P. Chin, D. R. Richardson, *Eur. J. Inorg. Chem.* **2003**, 1145–1156.
[10] P. V. Bernhardt, P. Chin, P. C. Sharpe, D. R. Richardson, *Dalton Trans.* **2007**, 3232–3244.
[11] J.-L. Schmitt, A.-M. Stadler, N. Kyritsakas, J.-M. Lehn, *Helv. Chim. Acta* **2003**, *86*, 1598–1624.
[12] J.-L. Schmitt, J.-M. Lehn, *Helv. Chim. Acta* **2003**, *86*, 3417–3426.
[13] K. M. Gardinier, R. G. Khoury, J.-M. Lehn, *Chem. Eur. J.* **2000**, *6*, 4124–4131.
[14] A.-M. Stadler, N. Kyritsakas, J.-M. Lehn, *Chem. Commun.* **2004**, 2024–2025.
[15] A.-M. Stadler, N. Kyritsakas, G. Vaughan, J.-M. Lehn, *Chem. Eur. J.* **2007**, *13*, 59–68.
[16] L. H. Uppadine, J.-P. Gisselbrecht, J.-M. Lehn, *Chem. Commun.* **2004**, 718–719.
[17] L. H. Uppadine, J.-M. Lehn, *Angew. Chem. Int. Ed.* **2004**, *43*, 240–243.
[18] M. Ruben, J.-M. Lehn, G. Vaughan, *Chem. Commun.* **2003**, 1338–1339.
[19] F. Loiseau, F. Nastasi, A.-M. Stadler, S. Campagna, J.-M. Lehn, *Angew. Chem. Int. Ed.* **2007**, *46*, 6144–6147.
[20] A.-M. Stadler, N. Kyritsakas, R. Graff, J.-M. Lehn, *Chem. Eur. J.* **2006**, *12*, 4503–4522.
[21] M. Barboiu, M. Ruben, G. Blasen, N. Kyritsakas, E. Chacko, M. Dutta, O. Radekovich, K. Lenton, D. J. R. Brook, J.-M. Lehn, *Eur. J. Inorg. Chem.* **2006**, 784–792.
[22] A.-M. Stadler, F. Puntoriero, S. Campagna, N. Kyritsakas, R. Welter, J.-M. Lehn, *Chem. Eur. J.* **2005**, *11*, 3997–4009.
[23] J. E. Beves, E. L. Dunphy, E. C. Constable, C. E. Housecroft, C. J. Kepert, M. Neuburger, D. J. Price, S. Schaffner, *Dalton Trans.* **2008**, 386–396.
[24] J. E. Beves, E. C. Constable, C. E. Housecroft, M. Neuburger, S. Schaffner, *Polyhedron* **2008**, in press.
[25] G. Lowe, A. S. Droz, T. Vilaiven, G. W. Weaver, L. Tweedale, J. M. Pratt, P. Rock, V. Yardley, S. L. Croft, *J. Med. Chem.* **1999**, *42*, 999–1006.
[26] G. Lowe, A. S. Droz, J. J. Park, G. W. Weaver, *Bioorg. Chem.* **1999**, *27*, 477–486.
[27] Z. Zhou, G. H. Sarova, S. Zhang, Z. Ou, F. T. Tat, K. M. Kadish, L. Echegoyen, D. M. Guldi, D. I. Schuster, S. R. Wilson, *Chem. Eur. J.* **2006**, *12*, 4241–4248.
[28] H. E. Gottlieb, V. Kotlyar, A. Nudelman, *J. Org. Chem.* **1997**, *62*, 7512–7515.
[29] *Rodd's Chemistry of Carbon Compounds*, 2nd ed. (Ed.: S. Coffey), Elsevier, Amsterdam, **1965**, vol. I, part B, pp. 68–71.
[30] A. L. Spek, *J. Appl. Crystallogr.* **2003**, *36*, 7–13.
[31] M. G. B. Drew, G. R. Willey, *J. Chem. Soc. Perkin Trans. 2* **1986**, 215–220.
[32] G. Tosi, L. Cardellini, G. Bocelli, *Acta Crystallogr., Sect. B* **1988**, *44*, 55–63.
[33] E. Chiba, K. Tani, M. Shuto, N. Haga, M. Tokonami, *Acta Crystallogr., Sect. C* **1990**, *46*, 414–417.
[34] M. Nagel, R. Allmann, *Cryst. Struct. Commun.* **1981**, *10*, 905–908.
[35] G. Tosi, P. Bruni, L. Cardellini, G. Bocelli, *Gazz. Chim. Ital.* **1984**, *114*, 111–115.
[36] M. G. B. Drew, M. J. Hudson, P. B. Iveson, M. L. Russell, J.-O. Liljenzin, M. Skålberg, L. Spjuth, C. Madic, *J. Chem. Soc., Dalton Trans.* **1998**, 2973–2980.
[37] C. J. Kepert, B. W. Skelton, A. H. White, *Aust. J. Chem.* **1994**, *47*, 391–396.
[38] C. Berthon, M. S. Grigoriev, *Acta Crystallogr., Sect. E* **2005**, *61*, o1216–o1217.
[39] I. A. Charushnikova, C. Den Auwer, *Russ. J. Coord. Chem.* **2004**, *30*, 511–519.
[40] K. N. Robertson, P. K. Bakshi, S. D. Lantos, T. S. Cameron, O. Knop, *Can. J. Chem.* **1998**, *76*, 583–611.
[41] M. G. B. Drew, P. B. Iveson, M. J. Hudson, J.-O. Liljenzin, L. Spjuth, P.-Y. Cordier, Å. Enarsson, C. Hill, C. Madic, *J. Chem. Soc., Dalton Trans.* **2000**, 821–830.
[42] W. Huang, H. Qian, *J. Mol. Struct.* **2007**, *832*, 108–116.
[43] A. Hergold-Brundić, Z. Popović, D. Matković-Calogović, *Acta Crystallogr., Sect. C* **1996**, *52*, 3154–3157.
[44] A. Kochel, *Acta Crystallogr., Sect. E* **2006**, *62*, m37–m38.
[45] See for example: G. R. Newkome, N. S. Bhacca, *J. Org. Chem.* **1971**, *36*, 1719–1720; A. F. Hegarty, P. J. Moroney, F. L. Scott, *J. Chem. Soc. Perkin Trans. 2* **1973**, 1466–1471.
[46] L. Lunazzi, C. Magagnoli, M. Guerra, D. Macciantelli, *Tetrahedron Lett.* **1979**, *20*, 3031–3032.
[47] F. Kaberia, B. Vickery, G. R. Willey, M. G. B. Drew, *J. Chem. Soc. Perkin Trans. 2* **1980**, 1622–1626.
[48] B. Vickery, G. R. Willey, M. G. B. Drew, *Acta Crystallogr., Sect. C* **1985**, *41*, 1072–1075.
[49] J. L. Cook, C. A. Hunter, C. M. R. Low, A. Perez-Velasco, J. G. Vinter, *Angew. Chem. Int. Ed.* **2007**, *46*, 3706–3709.
[50] See for example: G. J. Karabatos, R. A. Taller, *J. Am. Chem. Soc.* **1963**, *85*, 3624–3629, and ref.[47,48].
[51] E. Farkas, É. A. Enyedy, G. Micera, E. Garribba, *Polyhedron* **2000**, *19*, 1727–1736.
[52] *COLLECT Software*, Nonius BV, **1997**–**2001**.
[53] A. Altomare, G. Cascarano, G. Giacovazzo, A. Guagliardi, M. C. Burla, G. Polidori, M. Camalli, *J. Appl. Crystallogr.* **1994**, *27*, 435–435.
[54] XRED, v. 1.08, Stoe & Cie software, **1996**.
[55] G. M. Sheldrick, *SHELXS86*, Univ. of Göttingen, Germany, **1986**.
[56] Z. Otwinowski, W. Minor, *Methods in Enzymology*, vol. 276 (Eds.: C. W. Carter, R. M. Sweet Jr), **1997**, Academic Press, New York, pp. 307.
[57] P. W. Betteridge, J. R. Carruthers, R. I. Cooper, K. Prout, D. J. Watkin, *J. Appl. Crystallogr.* **2003**, *36*, 1487–1487.
[58] I. J. Bruno, J. C. Cole, P. R. Edgington, M. K. Kessler, C. F. Macrae, P. McCabe, J. Pearson, R. Taylor, *Acta Crystallogr., Sect. B* **2002**, *58*, 389–397.
[59] F. H. Allen, *Acta Crystallogr., Sect. B* **2002**, *58*, 380–388.

Received: March 20, 2008
Published Online: May 30, 2008

